

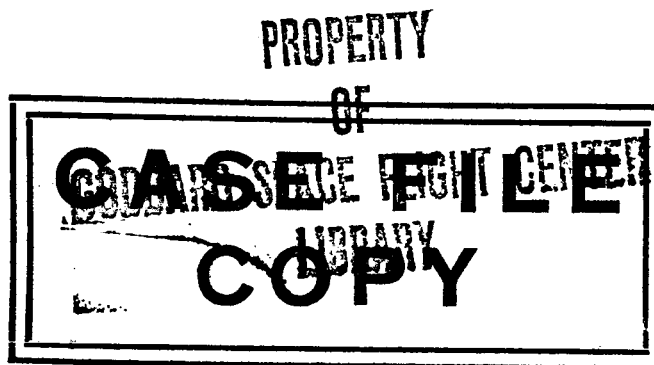
APOLLO

WDL-TR-EI45

22 May 1963

39769

AN EVALUATION OF OPTICAL METHODS
FOR TRACKING AND COMMUNICATIONS
IN SUPPORT OF APOLLO LUNAR MISSIONS



Submitted to the
NATIONAL AERONAUTICS AND SPACE ADMINISTRATION
MANNED SPACECRAFT CENTER
Houston, Texas

N67-85114

FACILITY FORM 802

(ACCESSION NUMBER)

69

(PAGES)

61-87168

(NASA CR OR TMX OR AD NUMBER)

(THRU)

None

(CODE)

(CATEGORY)

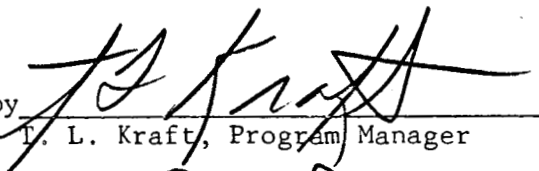
WDL TECHNICAL REPORT E-145

AN EVALUATION OF OPTICAL METHODS
FOR TRACKING AND COMMUNICATIONS
IN SUPPORT OF APOLLO LUNAR MISSIONS

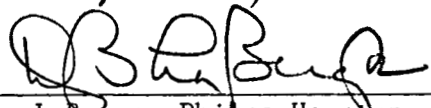
22 MAY 1963

Submitted to the
NATIONAL AERONAUTICS AND SPACE ADMINISTRATION
MANNED SPACECRAFT CENTER
Houston, Texas

Submitted by


T. L. Kraft, Program Manager

Approved by


W. B. Laberge, Philco Houston
Operations Manager

PHILCO CORPORATION
A Subsidiary of Ford Motor Company
Western Development Laboratories
Palo Alto, California

This study report which has been prepared under Contract NAS 9-366 is distributed for your information. The subject of this document should not be regarded as a firm Manned Spacecraft Center position nor should it commit the Manned Spacecraft Center. This document reflects the recommendations of the Philco Corporation as a result of their study effort.

FOREWORD

This is an engineering report based on studies being performed for the Manned Spacecraft Center, NASA, under contract NAS 9-366. The contract title is The Design and Development Study for Manned Space Flight Operations Control and Support. This report covers the results of one task and is being submitted in accordance with the requirements contained in the statement of Work in paragraph F.3. c(13) (c) dated February 1, 1963.

This report presents the results of the studies performed by Philco on the possible utilization of optical methods for tracking and communication in support of the lunar Apollo missions. The limited data available on the surface properties of the command and service modules and the lunar excursion module made it necessary to present the results in parametric form. Consequently, final conclusions cannot be drawn. The data presented does, however, adequately summarize the capabilities and potential of optical techniques against RF methods for tracking and communication. It is recommended that further studies be performed when the engineering specifications on the "skins" of the Apollo vehicles are complete.

TABLE OF CONTENTS

<u>Section</u>		<u>Page</u>
1	INTRODUCTION	
	1.1 General	1-1
	1.2 Comparison of Optical and Radio Techniques.	1-1
	1.3 Advantages of Optical Systems	1-3
	1.4 Disadvantages of Optical Observations	1-6
2	TARGET DETECTION	
	2.1 Vehicle Brightness.	2-1
	2.2 Background Brightness	2-11
	2.3 Detection Thresholds.	2-13
	2.4 Brightness of Other Sources	2-45

LIST OF ILLUSTRATIONS

<u>Figure</u>		<u>Page</u>
1	Comparison of Blackbody Radiation from Three Sources and Atmospheric Transmission	1-2
2	The Instantaneous Probability that a Satellite at a Given Altitude is in Eclipse.	1-8
3	Apollo Spacecraft Configuration (Approximate Dimensions)	2-2
4	Lunar Excursion Module (Approximate Dimensions).	2-3
5	Geometry of Reflection from a Cylinder	2-5
6	Variation of Brightness with Phase Angle	2-9
7	Maximum Brightness at Phase Angle 87° of an Individual Module	2-10
8	Background Brightness.	2-12
9	Mean Brightness of The Moon.	2-14
10	Variation in Threshold of the Human Eye with Background Brightness and Target Size.	2-15
11	Variation of Threshold of the Human Eye.	2-16
12	Response of the Pupil of the Eye to Brightness Level	2-19
13	Limiting Magnitudes of Visual Telescopes with $M = 16$ D Inches, Moderate Ease of Certain Detection 3 Second of Arc Seeing Disk Diameter . .	2-21
14	Limiting Magnitudes of Photographic Telescopes . .	2-27
15	Photon Flux Through an Aperture from a 6000°K $m_v = 0.0$ Source	2-31
16	Performance of Image Tubes Against a Dark Sky with 20-inch Aperture, $f/12$	2-39

LIST OF ILLUSTRATIONS (CONT'D)

<u>Figure</u>		<u>Page</u>
17	Limiting Magnitudes of Various Saturated Detectors.	2-44
18	Radius and Mass of a Thin Film Inflatable Sphere as a Function of Brightness	2-46
19	Brightness of a 45-inch Diameter Flat Mirror as a Function of Distance	2-50

LIST OF TABLES

<u>Table</u>		<u>Page</u>
I	Comparison of Optical and Radio Tracking and Communication Equipments	1-11
II	Values of the Resolution of Image Converters as a Function of Integration Time When Exposed to a Moonless Night Sky.	2-37
III	Threshold Magnitudes of Image Tubes, 20-inch f/12 Telescope	2-38

SECTION 1

INTRODUCTION

1.1 GENERAL

The purpose of this report is to summarize the capabilities of optical methods for data acquisition and communication as backup to radio methods for the support of the Apollo lunar missions.

As dictated by the mission control concept, the role of the GOSS is essentially to back up the spacecraft from an information standpoint.

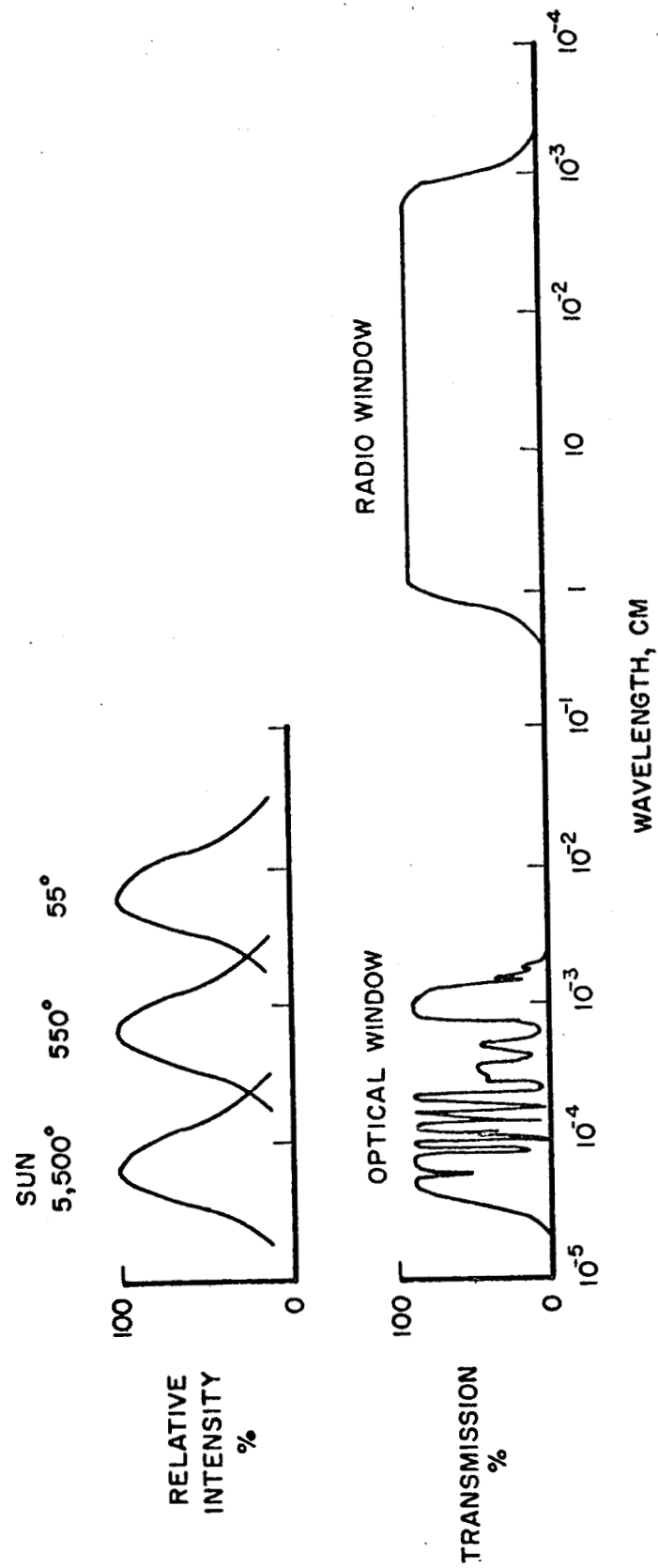
As thus defined, the potential usefulness of optical ground equipments lies in the areas of navigation (tracking) backup and communication.

This report does not consider the very important pre-launch application of optical techniques to the alignment of the launch vehicle.

1.2 COMPARISON OF OPTICAL AND RADIO TECHNIQUES

Because of atmospheric absorption, only two major regions of the spectrum are available for communication between the spacecraft and the surface of the Earth: The optical "window", extending from 2900 Å to about 7000 Å and the radio "window", extending from approximately 1 cm. to approximately 10 meters (Figure 1).

In the infrared region beyond 7000 Å, there are a number of less prominent "windows", the most important of which is in the vicinity of 10 microns. Observations of the spacecraft from the ground and communications between the spacecraft and the ground are restricted to operation within one or more of these windows if infrared methods are used. Generally, the "window" in the vicinity of 10 microns is most often used.



A-164.

Fig. 1 Comparison of Blackbody Radiation from Three Sources and Atmospheric Transmission

1.3 ADVANTAGES OF OPTICAL SYSTEMS

Figure 1 indicates an important advantage of operating at optical frequencies; namely, the availability of natural sources of energy. By far the most important natural source of illumination for the spacecraft is the Sun, which radiates 98% of its energy in the wavelength region 3,000 - 40,000 Å. The total intensity of the Sun's radiation just outside the earth's atmosphere is about $1.4 \times 10^6 \text{ erg cm}^{-2} \text{ sec}^{-1}$. The spacecraft itself also radiates because of its temperature, which may be expected to be in the vicinity of a few hundred degrees absolute. Thus, the majority of the blackbody spacecraft radiation will be in the region of the 10 micron window. For a vehicle with a 100% emissivity and a temperature between 100 and 500 °K, the total energy emitted will range between 6×10^3 and $4 \times 10^6 \text{ erg cm}^{-2} \text{ sec}^{-1}$. From considerations of the thermal engineering of a vehicle, and because of the smaller window through which it may be observed, it is reasonable to anticipate that the amount of energy reaching the earth's surface due to the thermal radiation of the spacecraft will be of the same order as or less than the reflected solar radiation. Since the illumination of the spacecraft by other sources is relatively low, insofar as tracking is concerned, the vehicle must be artificially illuminated to be observed in the "radio" region.*

*The effect of solar radiation reflected from, and thermal emission of, the Earth is significant for vehicles with altitudes less than about 1000 KM. However, since for the majority of the Apollo Lunar Mission this altitude is exceeded, the effect of this source of illumination is unimportant.

Therefore, it is readily apparent that an optical system utilizing reflected sunlight or the thermal emission of the spacecraft offers certain advantages, energywise, over a radio system. This matter is more thoroughly discussed in Section 2.

Another advantage of optical systems lies in their intrinsically greater resolution. Radio and optical instruments are fundamentally limited by the wave nature of radiation. The minimum angle of resolution varies directly with the wavelength and inversely with the aperture. As typical values of the wavelengths of primary interest, we may consider 5×10^{-5} cm. corresponding to the visible region of the spectrum, 10^{-3} cm. corresponding to the 10μ window, and 15 cm. corresponding to a 2 KMC radar. It follows that the ratio of apertures required to achieve the same angular resolution at these three wavelengths is $1:20:3 \times 10^5$. As an example, an optically perfect 40-inch aperture telescope operating under ideal conditions could resolve an object 0.14 seconds of arc in diameter (roughly the angle subtended by one foot at a distance of 240 nautical miles). To perform the same operation in the radio region of the spectrum, one would require a dish antenna with an aperture of 164 nautical miles. This property of a narrow attainable beamwidth and the absence of side lobes results in an optical communication system which offers increased security and reduced susceptibility to jamming and interference, as compared to a conventional radio system. Resolution is much less important than one might suppose at first sight for purposes of accurate determination of the direction to an isolated point source (one can find the center of a baseball or a ball bearing with comparable accuracies). Resolution does become

important, however, when determining the relative positions of two apparently close objects, as in the final stages of a rendezvous.

Aside from the question of resolving power, consideration must also be given to the pointing accuracy and repeatability of the instrument. In other words, attention must be paid to the facility with which the observations may be reduced to a fundamental reference frame. An advantage of determining directions by observations at optical frequencies lies in the availability of a stellar reference frame at these frequencies. The large number of stars with accurately determined directions not only provides a convenient method for calibrating optical metric equipment, but also allows angular measurements to be made differentially. Thus, precision optical positional measurements can be made in such a way as to not rely heavily on the pointing accuracy or repeatability of the instrument. This is not the case with radar equipments.

In high precision direction determination, atmospheric effects are quite important, both at optical and radar frequencies. For the visible and infrared regions, only the normal index of refraction of a neutral gas must be considered in the reduction of the observations. In the radio region, however, ionization is dominant, and the effect upon observations is about five times larger and much more variable. Not only is the correction for refraction much less in the optical case, but, as just mentioned, differential measurements may be made which almost eliminate the effects of refraction by the very nature of the observations.

A few examples of the accuracies of present equipment may prove informative. Modern precision radars, for example the FPS-16, have an accuracy

in the field of about 20 seconds of arc. Present optical trackers (not using a stellar reference frame) are about twice as accurate, while instruments using star backgrounds reach, in missile range operation, one or two seconds of arc accuracy. Somewhat improved fundamental (absolute) accuracies are readily obtained with astronomical instruments, while relative positions accurate to a few hundredths of a second of arc can be obtained from a series of long focal-length astrometric observations.

An often quoted advantage of optical systems is that they are small, relatively inexpensive and portable. As will be seen later, not all of the phases of the Apollo Lunar Mission can be adequately covered by small easily portable equipments.

1.4 DISADVANTAGES OF OPTICAL OBSERVATIONS

The principal disadvantage of optical methods is their greater dependence on the weather. To overcome the difficulties imposed by inclement weather, either duplicate observing stations or highly portable equipment must be employed.

Another serious disadvantage of optical systems lies in the variation of background brightness, or target contrast, due to the changing brightness of the sky. In the course of a day, the sky background varies through a range in brightness of about 10^8 . For an ideal detector, this corresponds to a variation in the noise equivalent signal by a factor of 10^4 . Everything else being constant, the change in sky illumination from day to night therefore results in a variation in target range for a solar, or

self-illuminated target, by a factor of 100. In practice, this variation will usually be larger.

If the source of illumination of the vehicle is the sun, consideration must be given to the effect of eclipses on the efficiency of individual sensors. The earth's shadow is no serious obstacle to the detection and tracking of spacecraft at a distance of several earth radii.* For very close satellites, as the spacecraft will be during the earth orbit phase of the mission, the earth's shadow becomes a serious problem, particularly if observations are limited to the hours of darkness.

Figure 2 indicates the probability that an individual satellite is in an eclipse, assuming a uniformly distributed satellite population. The figure also displays the maximum duration of an eclipse as a function of altitude for vehicles traveling in circular orbits. For optical tracking during the earth-orbit phase of the mission, either an extensive sensor network is required, or else tracking must be accomplished during daylight hours or by some means other than solar illumination. It is still possible, of course, that the spacecraft may be observed in the infrared region because of its natural thermal emission.

Optical techniques for the measurement of range and range-rate are at a severe disadvantage as compared to radar methods, despite the fact that optical radars, utilizing lasers, show considerable promise. For the

*It is assumed that the mission will be conducted in such a way that the spacecraft will not be in eclipse during the transit phase, nor that an eclipse of the moon will occur during the lunar landing.

A-166

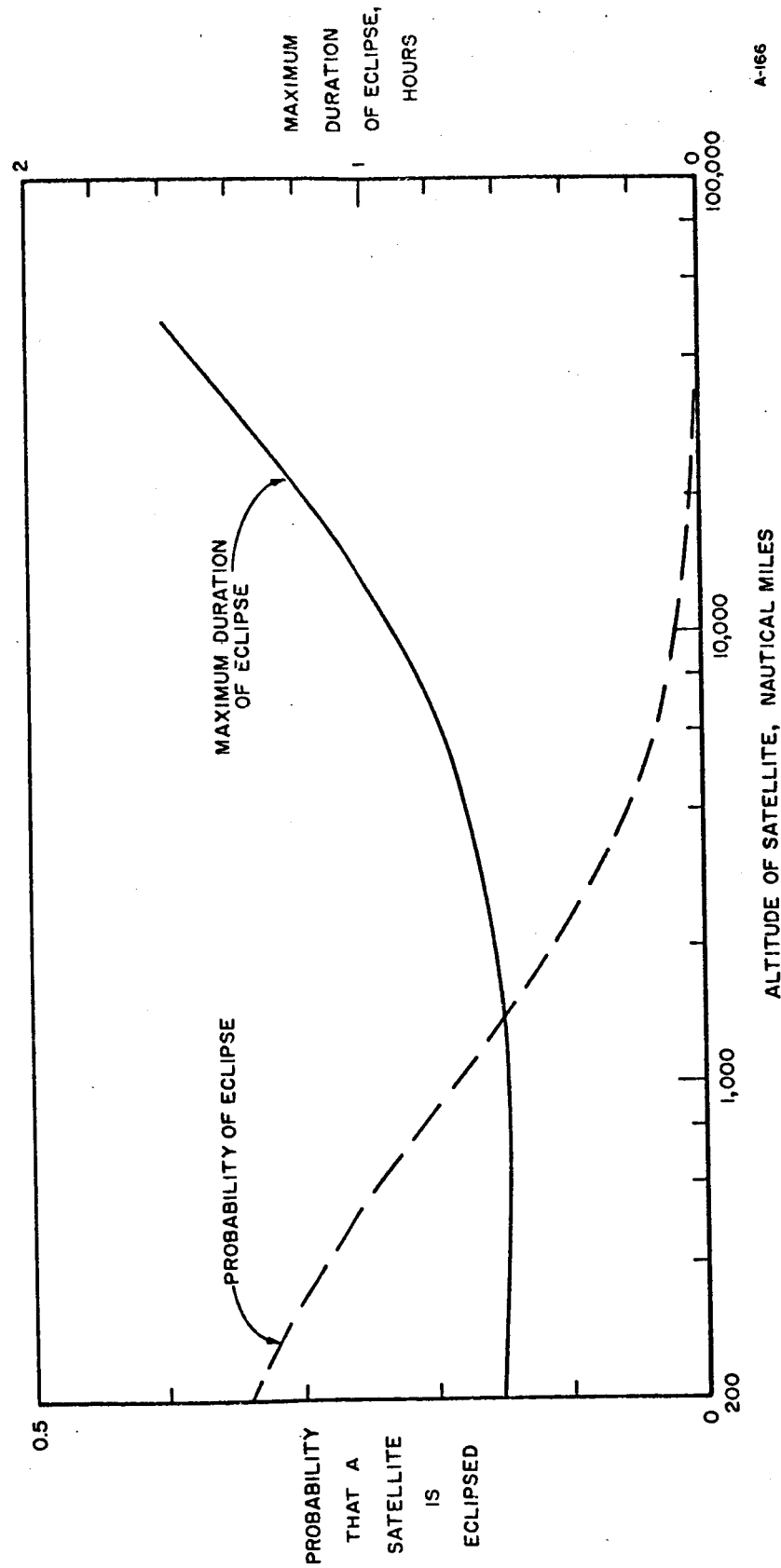


Fig. 2 The Instantaneous Probability that a Satellite at a Given Altitude is in Eclipse (for a uniform distribution of satellites) and the Maximum Duration of Eclipse (for circular orbits) as a Function of Satellite Altitude

reasons previously given, range determination by triangulation is best accomplished by optical methods. Unlike echo ranging, which is essentially limited in accuracy by timing accuracy (and by our knowledge of the velocity of propagation), and may therefore be expected to have a relatively constant percentage range uncertainty, the percentage error in triangulation measurements, being limited by the precision with which small angles can be measured, increases rapidly with the range. Nevertheless, a probable error in the range of 10 to 20% can be obtained at ranges up to 2.5×10^6 times the base line between the two stations forming the triangulation network. As the parallax at such a range would amount to only 0.04 seconds of arc, and the parallax error, about ± 0.005 seconds of arc, it is apparent that a large series of precision observations with a pair of long-focal length instruments would be required for this purpose. The problem is further complicated by the motion of the target. Furthermore, such precision triangulation would prove difficult as far as implementation with a short-time readout is concerned.

Radial velocities (range rates) may be observed by either noting the change in range per unit time or by measuring the Doppler shift of radiation reflected from the vehicle. The first of these methods is simply a logical extension of the range measuring methods already mentioned, and is therefore best restricted to radar. The range accuracies of present radars, however, limit the accuracy of the radial velocity determined in this manner to something on the order of a few miles per unit time. A far more accurate determination of radial velocity may be made by Doppler techniques, since, for a given velocity, the percentage wavelength change is a constant,

observations at the longer wavelengths will take advantage of the larger absolute wavelength change. Present radar is capable of providing range rate data accurate to within a few feet per second. Optical systems may be expected to perform this function with at least an order of magnitude poorer accuracy.

A final disadvantage of optical techniques which will be mentioned lies in the method of securing observations of the highest angular accuracy. As already mentioned, this is done by differential measurement with respect to a stellar reference frame. Most generally, this is done photographically. The procedures most widely employed at present result in considerable time delays between observation and reduction.

Table I summarizes the preceding comparison of optical and radio techniques.

TABLE I

COMPARISON OF OPTICAL AND RADIO
TRACKING AND COMMUNICATION
EQUIPMENTS

EQUIPMENT TYPE		OPTICAL		RADIO
		Visible	Infrared	
Fundamental Properties	Source of energy	Ambient (sunlight) or artificial	Ambient (thermal) or artificial	Artificial
	Angular resolution	Very high: Resolution of small detail and secure communication possible	High	Low
	Angular accuracy	Very high: Accurate reference frame available; moderate and easily calibrated refraction errors	Moderate	Low: Lack of accurate external reference; large and variable poorly calibrated refraction errors.
	Range accuracy	Except for lasers, which require development, low	As given for visible	High
	Range Rate accuracy	Low	Low	Doppler shift equipments very high, otherwise low
Interference	Background illumination	Extremely variable	Relatively constant, at most frequencies	As given for infrared
	Weather	An extreme problem	As given for visible	A problem only at some frequencies
	Earth Shadow	A problem only for solar illuminated objects at low altitudes	Relatively unimportant	Unimportant
SYSTEM CONSIDERATIONS		Near real-time delivery of highly accurate angles a program. Some equipments portable. Considerable network already established.	Some equipments portable	Considerable network already established

SECTION 2

TARGET DETECTION

2.1 VEHICLE BRIGHTNESS

Brightness by Reflected Light

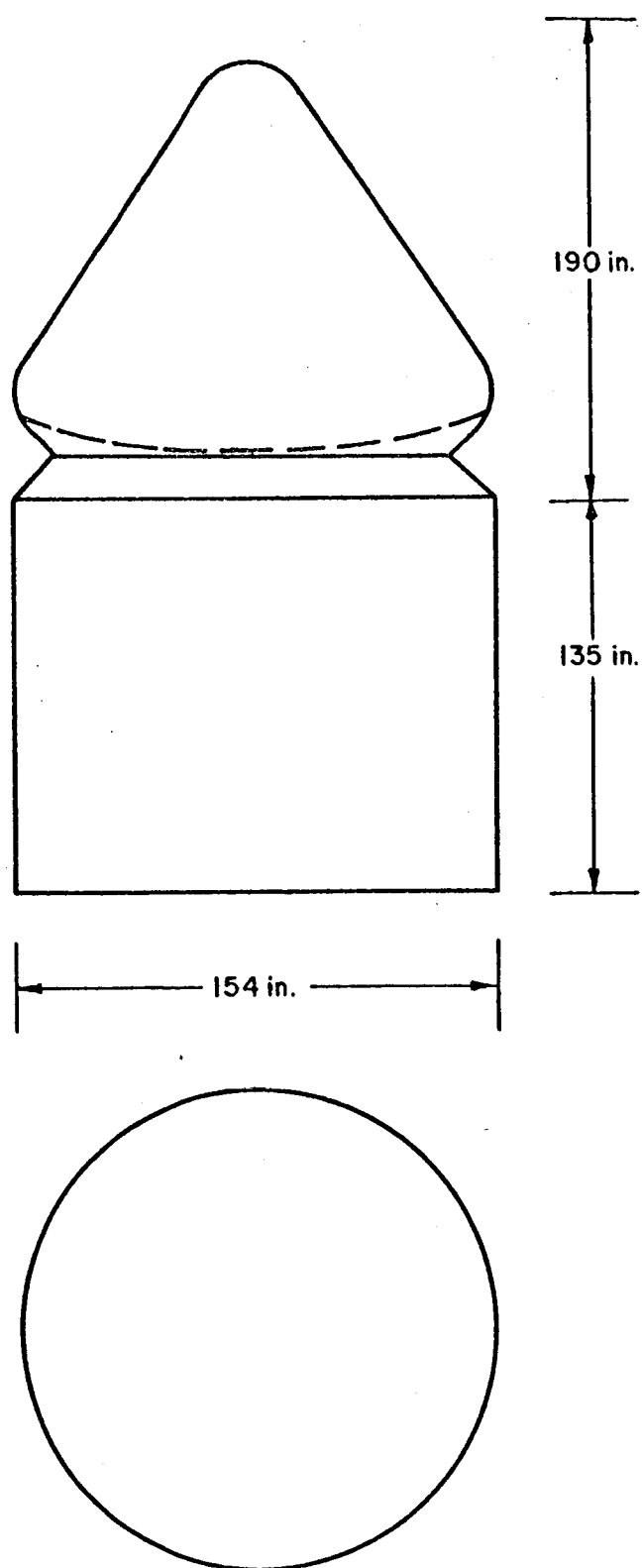
Figures 3 and 4 show the probable configuration of the Apollo spacecraft and the lunar excursion module (LEM). Lack of knowledge of the surface compositions of these vehicles, and the extreme complexity of the latter vehicle, make an accurate estimate of the brightnesses of the vehicles impossible. For the purpose of making a preliminary brightness estimate, the vehicles have been considered to be described in terms of the following elements:

- a. The spacecraft is considered to be a diffusely reflecting cylinder 154 inches in diameter and 135 inches long capped on one end by the re-entry vehicle.
- b. The re-entry vehicle is considered to be a diffusely reflecting cone 154 inches in diameter and 190 inches long, closed at its larger dimension with a flat plate.
- c. The lunar excursion module is considered to be a diffusely reflecting cylinder 125 inches in diameter and 140 inches in length, closed at both ends by a flat plate.

A diffusely reflecting cylinder has an apparent radiant intensity,

J_{cyl} , given by

$$(1) \quad J_{cyl} = \frac{Y}{\pi} H_{\odot} \left[\frac{r l}{2} \right] \left[\left\{ (\pi - \epsilon) \cos \epsilon + \sin \epsilon \right\} \sin \phi_{\odot} \sin \phi_{obs} \right],$$



A-167

Fig. 3 Apollo Spacecraft Configuration
(Approximate Dimensions)

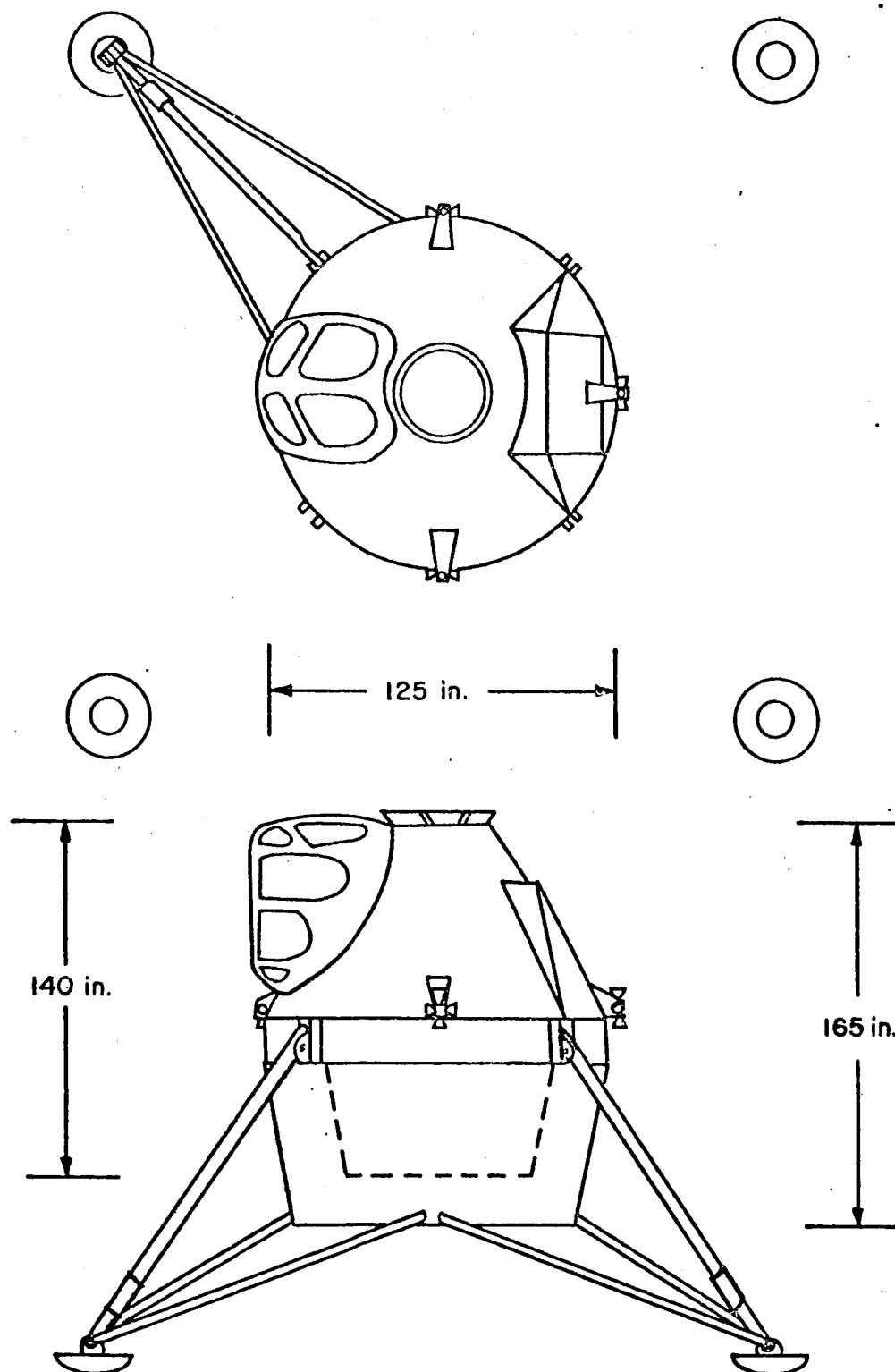


Fig. 4 Lunar Excursion Module
(Approximate Dimensions)

A-165

where

γ is the reflectance of the vehicle,

H_{\odot} is the solar irradiance,

r and l are the radius and length of the cylinder,

ϕ_{\odot} and ϕ_{obs} are the angles from the cylinder axis to the direction of the sun and the observer.

and

$$\cos \epsilon = \frac{\cos \beta - \cos \phi_{\odot} \cos \phi_{\text{obs}}}{\sin \phi_{\odot} \sin \phi_{\text{obs}}},$$

where β is the phase angle (Figure 5). By way of comparison, the apparent radiant intensity of a diffusely reflecting sphere is given by

$$(2) \quad J_{\text{sphere}} = \frac{\gamma}{\pi} H_{\odot} \left[\frac{2}{3} r^2 \right] \left[(\pi - \beta) \cos \beta + \sin \beta \right].$$

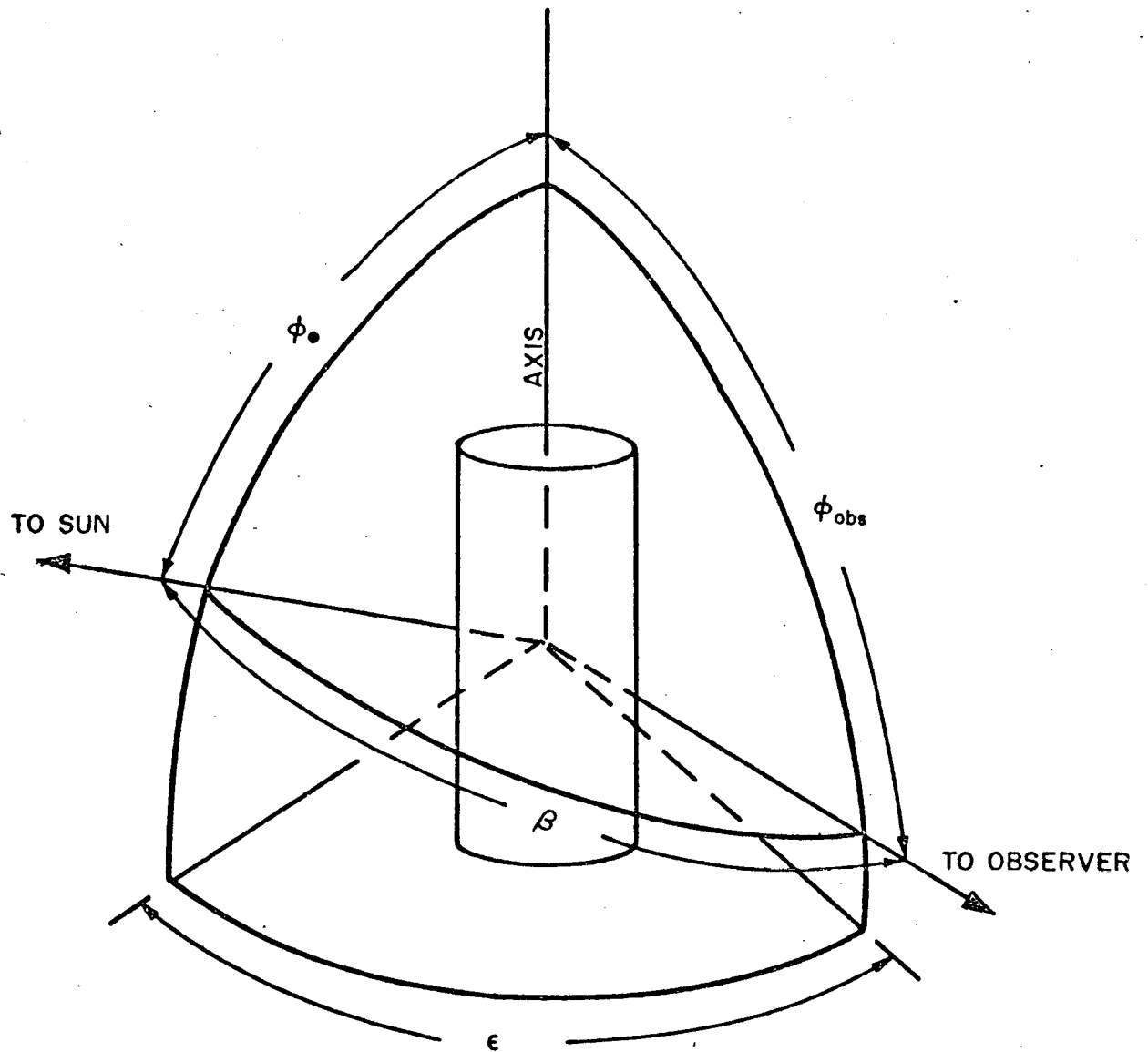
Maximum brightness of the cylinder requires that $\phi_{\odot} = \phi_{\text{obs}} = \pi/2$ and that $\beta = 0$. If we only require the first of these assumptions,

$$\phi_{\odot} = \phi_{\text{obs}} = \frac{\pi}{2},$$

(3)

$$J_{\text{cyl}} = \frac{\gamma}{\pi} H_{\odot} \left[\frac{rl}{2} \right] \left[(\pi - \beta) \cos \beta + \sin \beta \right]$$

That is, when the directions to the sun and to the observer are both at right angles to the axis of the cylinder, the cylinder's brightness



A-168

Fig. 5 Geometry of Reflection from a Cylinder

as a function of phase angle is the same as that of a diffusely reflecting sphere with a radius given by

$$(4) \quad r = \sqrt{\frac{3}{4} r l} = 0.866 \sqrt{r l} .$$

Equations analogous to equation (1) may be developed for a diffuse cone.¹ For the special case of equation (3), the intensity of a cone is given by

$$\phi_{\bullet} = \phi_{\text{obs}} = \frac{\pi}{2} ,$$

(5)

$$J_{\text{cone}} = \frac{Y}{\pi} H_{\bullet} \left[\frac{r l \cos \alpha}{4} \right] \left[(\pi - \beta) \cos \beta + \sin \beta \right]$$

where α is the generating angle of the cone. For the cone of interest, $\alpha \sim 30^{\circ}$, and the cone's brightness as a function of phase angle is the same as that of a diffusely reflecting sphere with a radius given by

$$(6) \quad r = \sqrt{\frac{3 \sqrt{3}}{16} r l} = 0.57 \sqrt{r l} .$$

¹ See, for example, T. P. Fahy, "Astro-Optical Tracker Study," AFGC-TR-60-42, Perkin Elmer Corporation, 16 March 1960.

It will prove convenient to express the apparent brightnesses of the vehicles in stellar magnitudes. Taking the dimensions of the object in inches, and the range, ρ , in nautical miles, the apparent magnitude of a diffuse sphere is given by

$$(7) \quad m = m_{\odot} + 24.3 + 5 \log_{10} \rho - 2.5 \log_{10} \gamma r^2 \\ - 2.5 \log_{10} \left[\frac{2}{3\pi} \left\{ (\pi - \beta) \cos \beta + \sin \beta \right\} \right],$$

where m_{\odot} is the apparent magnitude of the sun (-26.8 on the visual scale). For the special case of $\phi_{\odot} = \phi_{\text{obs}} = \pi/2$, the apparent magnitudes of a cylinder and a cone may be calculated by use of the relationships (4) and (6).

Before proceeding, however, it is well to consider the effects of phase angle. For a specularly reflecting sphere, the expression analogous to equation (7) is

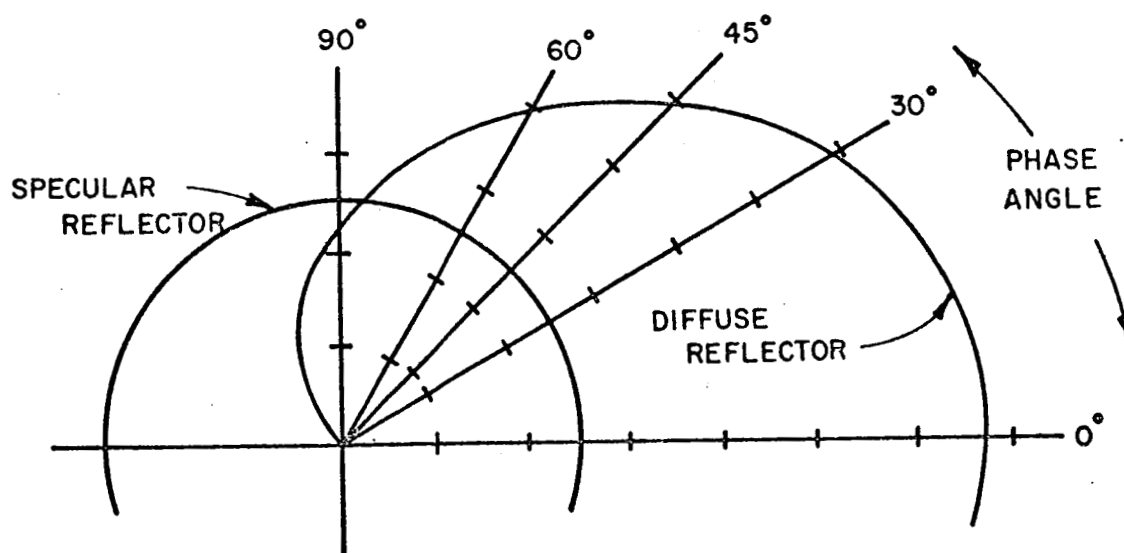
$$(8) \quad m = m_{\odot} + 24.3 + 5 \log_{10} \rho - 2.5 \log_{10} \gamma r^2 + 1.5.$$

It is to be noted that the magnitude of a specularly reflecting satellite is entirely independent of its phase angle, whereas the magnitude of a diffusely reflecting satellite does depend upon the relative positions of the sun, satellite and observer. Consequently, there will be certain ranges of phase angle where one type of reflector will have an advantage over the other.

Consider two satellites, one visible by sunlight reflected specularly and the other by diffuse reflection. They each have the same radius, albedo, and distance from the observer. Their variation of apparent brightness with phase angle is then shown by Figure 6. It is seen that the apparent brightness of a diffusely reflecting satellite between full phase and quadrature is greater than that of a similar satellite visible by specular reflection, becoming 2.66 times greater at opposition. But, from quadrature to inferior conjunction, the apparent brightness of the diffuse reflector decreases rapidly, and a satellite with specular reflection is definitely an advantage. The two types of reflectors are equal in apparent brightness at a phase angle of about 87° . For a preliminary design estimate, this phase angle has been adopted.

Figure 7 indicates the apparent brightness of the vehicles, on the basis of the model outlined above, as a function of range, for assumed overall reflectances between 30% and 100%. The three modules are all within 0.1 magnitude of each other, when considered under the above given conditions. Taken together, two of the vehicles would appear 0.75 magnitude brighter than the curves, while all three would appear 1.2 magnitudes brighter.

At ranges up to a few thousand nautical miles, the vehicles would be visible to the naked eye against a night-sky at maximum brightness. Beyond this distance, optical aid would be required. In the vicinity of the moon, distinguishing the vehicle above the background illumination presents a problem.



A-170

Fig. 6 Variation of Brightness with Phase Angle

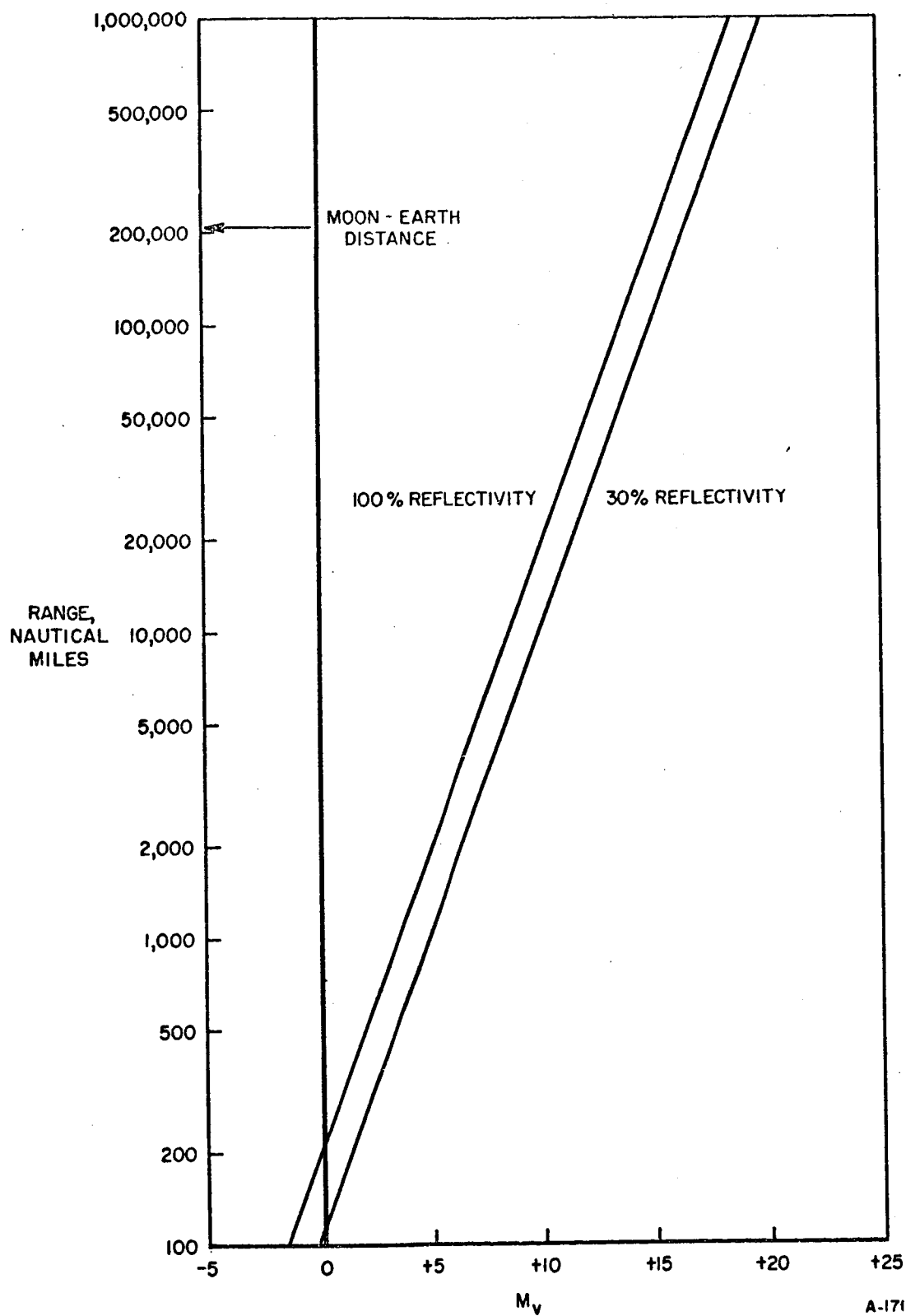


Fig. 7 Maximum Brightness at Phase Angle 87° of an Individual Module

The above results are, of course, tentative. It would be desirable to investigate the photometric properties of the vehicles in a laboratory using small scale models, once the configuration and surfacing parameters have been set.

Atmospheric extinction acts to reduce the range at which a target is visible. The total change in intensity due to extinction is not only one of quantity, but one of quality as well. Under average conditions, the zenithal extinction is about $0^m.2$ in yellow light and $0^m.4$ in blue. At a zenith distance of 60° , the air mass has doubled, and therefore the magnitude extinction runs about $0^m.4$ to $0^m.8$. The range on a self-or-solar-illuminated target observed at $Z = 60^\circ$ is thus reduced by a factor of between 2 and 4 by extinction depending on whether the observations are conducted in yellow or blue light, respectively, compared to the range computed neglecting extinction.

2.2 BACKGROUND BRIGHTNESS

Figure 8 indicates the variation in sky background brightness. The curves for the twilight sky were derived from the data of Koomen et al.² The data for the moonlit sky is due to Dole,³ based on a theoretical interpretation of the solar aureole. As has already been pointed out in the introduction, the brightness of the sky varies by a factor of 10^8 between night and day.

²Koomen, et al "Measurements of the Brightness of the Twilight Sky," Journal of the Optical Society of America, 42, 353, 1952.

³S. H. Dole, "Visual Detection of Light Sources on or near the Moon," ASTIA Document AD 133032, 27 May 1957. Rand Memorandum RM-1900.

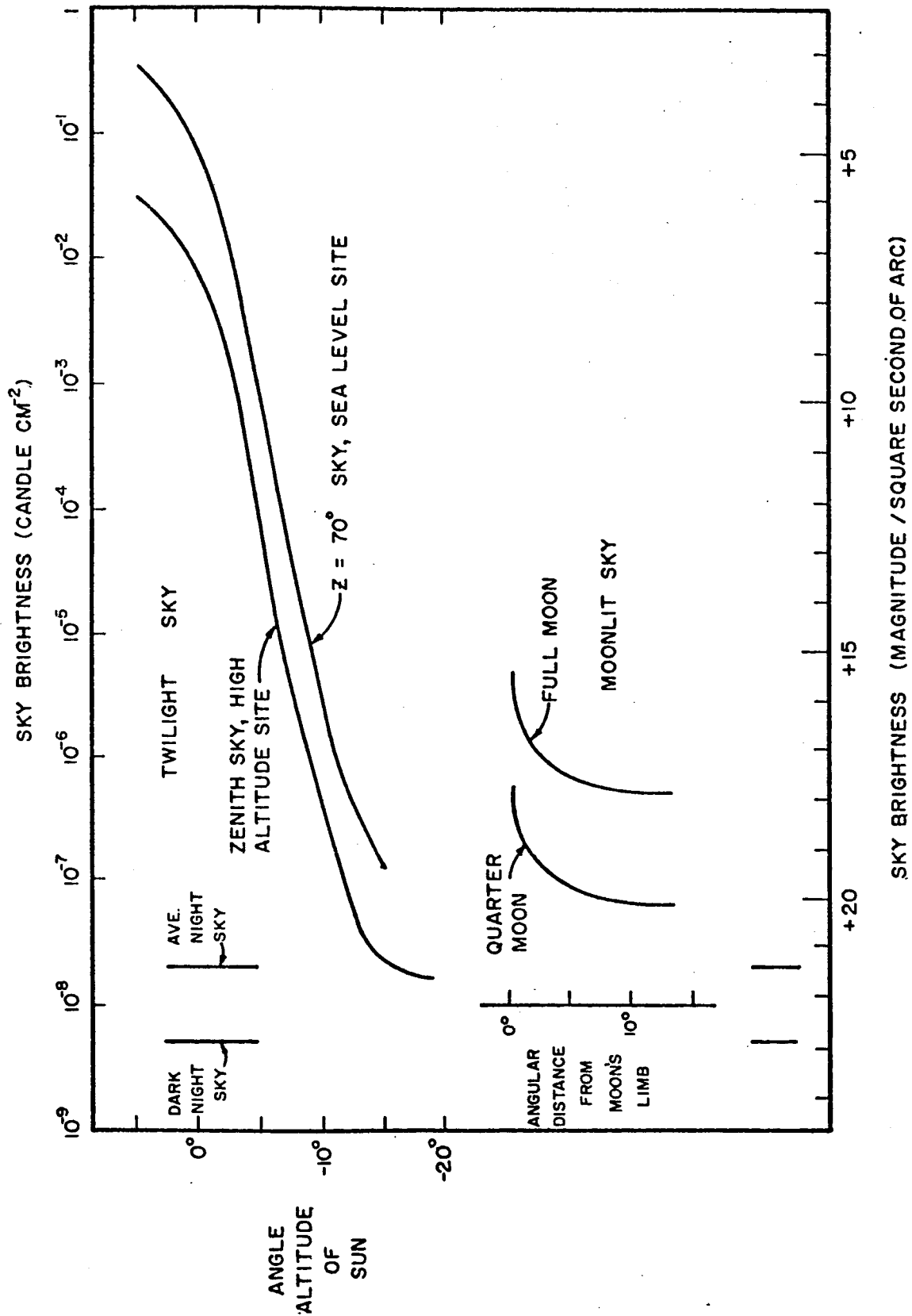


Fig. 8 Background Brightness

Figure 9 displays the brightness of the moon as a function of phase angle. The data, after Russell et al⁴, are a mean of both waxing and waning phases. More accurate data are available for specific areas of the moon, and for a final analysis, should be employed.

Light that is reflected from the earth onto the dark moon is another source of background brightness which should be considered in a more detailed analysis. This illumination is, of course, greatest at new moon, and for the present discussion will be neglected.

2.3 DETECTION THRESHOLDS

a. The Eye

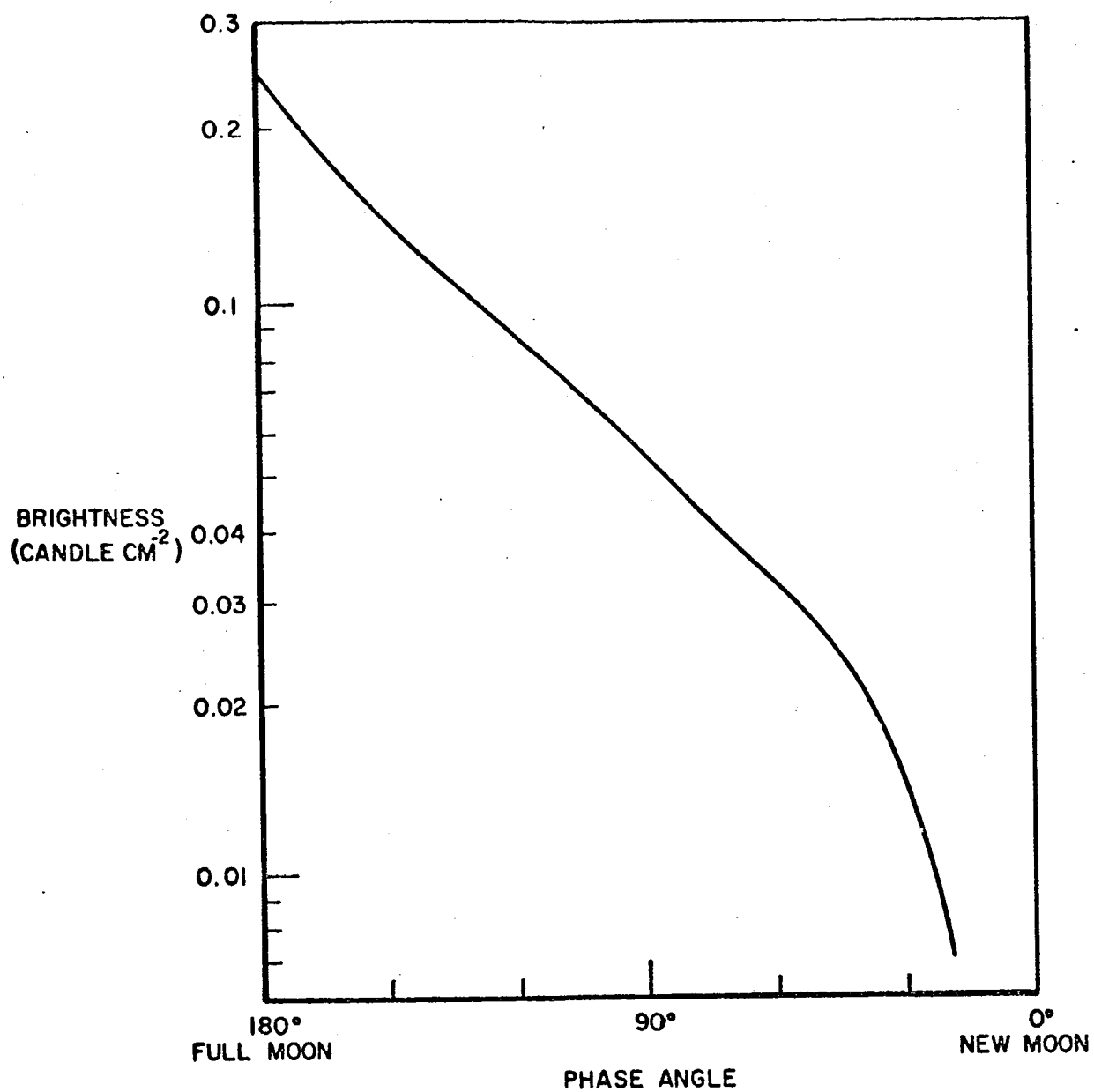
Typical of all "panoramic" detectors, the ability of the eye to detect a faint object against a luminous background depends on the angular extent of the object, its brightness, and the brightness of the background. Figure 10, based on the reduction of H. R. Blackwell's data⁵ by Tousey and Hulburt⁶, indicates these dependences for a 98% probability of detection. Figure 11 presents the same data in a different form.

The effect of a telescope on the detection of a faint source can be derived from optical principles. Following the notation of Tousey and Hulburt⁶, let

⁴Russell, Dugan, and Stewart, Astronomy, (Ginn and Co., New York), 1926, page 173.

⁵H. R. Blackwell, Journal of the Optical Society of America, 36, 624, 1946.

⁶R. Tousey and E. O. Hulburt, "The Visibility of Stars in the Daylight Sky," Journal of the Optical Society of America, 38, 886, 1948



A-169

Fig. 9 Mean Brightness of The Moon

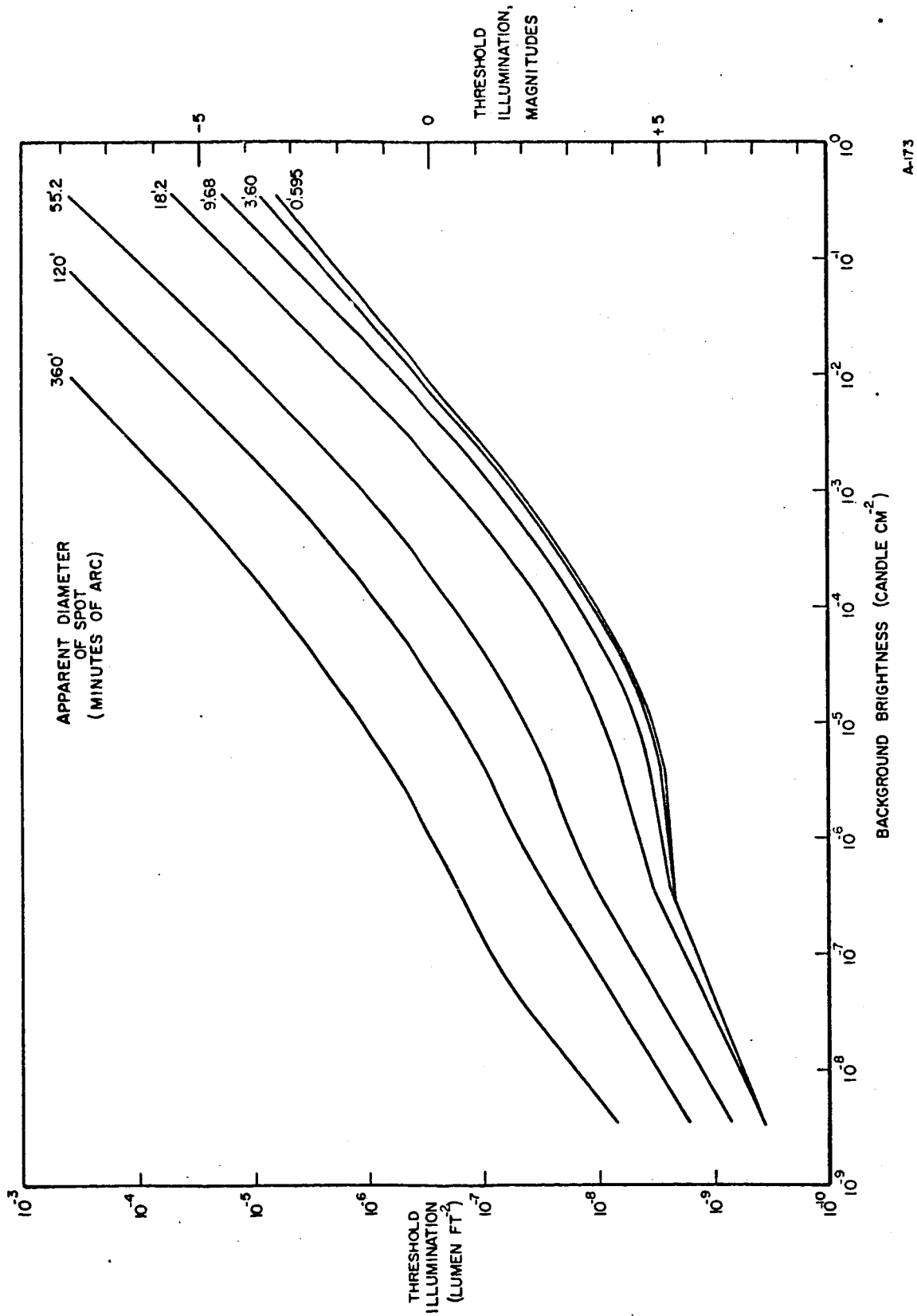


Fig. 10 Variation in Threshold of the Human Eye With Background Brightness and Target Size

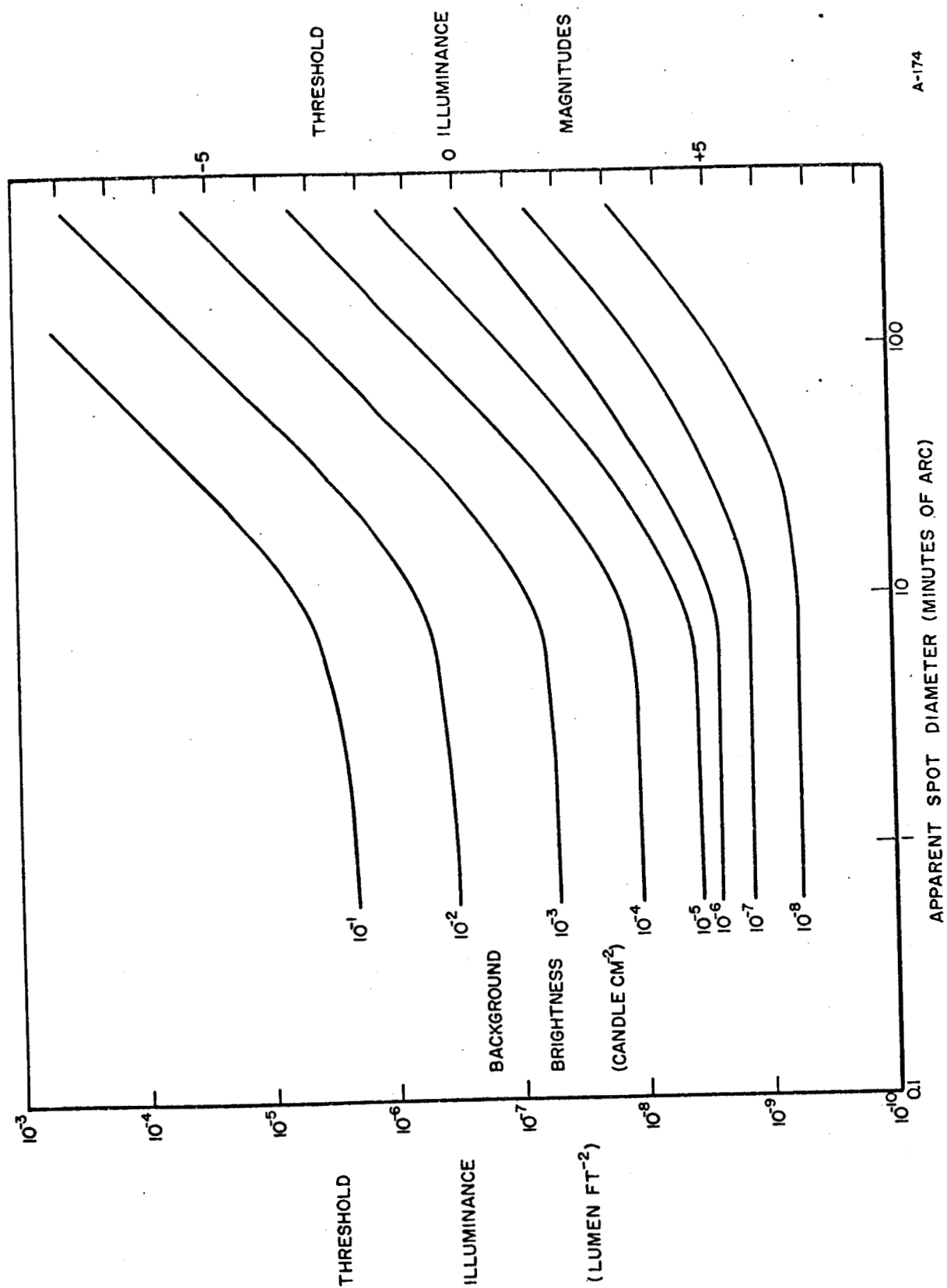


Fig. 11 Variation of Threshold of the Human Eye

D = the diameter of the objective (entrance pupil)

d = the diameter of the exit pupil

p = the diameter of the pupil of the eye

M = the magnification = D/d

t = the transmission of the telescope

i = stellar illumination

i_a = apparent stellar illumination when viewed
through the telescope

b = background brightness

b_a = apparent background brightness when viewed
through the telescope.

Then, for

$$d \geq p,$$

$$(9) \quad i_a = t M^2 i$$

$$(10) \quad b_a = t b$$

and for

$$d \leq p,$$

$$(11) \quad i_a = t (D/p)^2 i$$

$$(12) \quad b_a = t (d/p)^2 b = t (D/pM)^2 b.$$

It should be clear that to detect a faint point source, we desire $d \leq p$ and a large magnification. On the other hand, there is a limit to what can be accomplished by increased magnification, before the effect illustrated in Figures 10 and 11 becomes important. We might note here that

Fahy¹ considered the case $d \geq p$, while considering this effect, and that Dole³ considered the case $d \leq p$, without taking into account this increase in threshold.

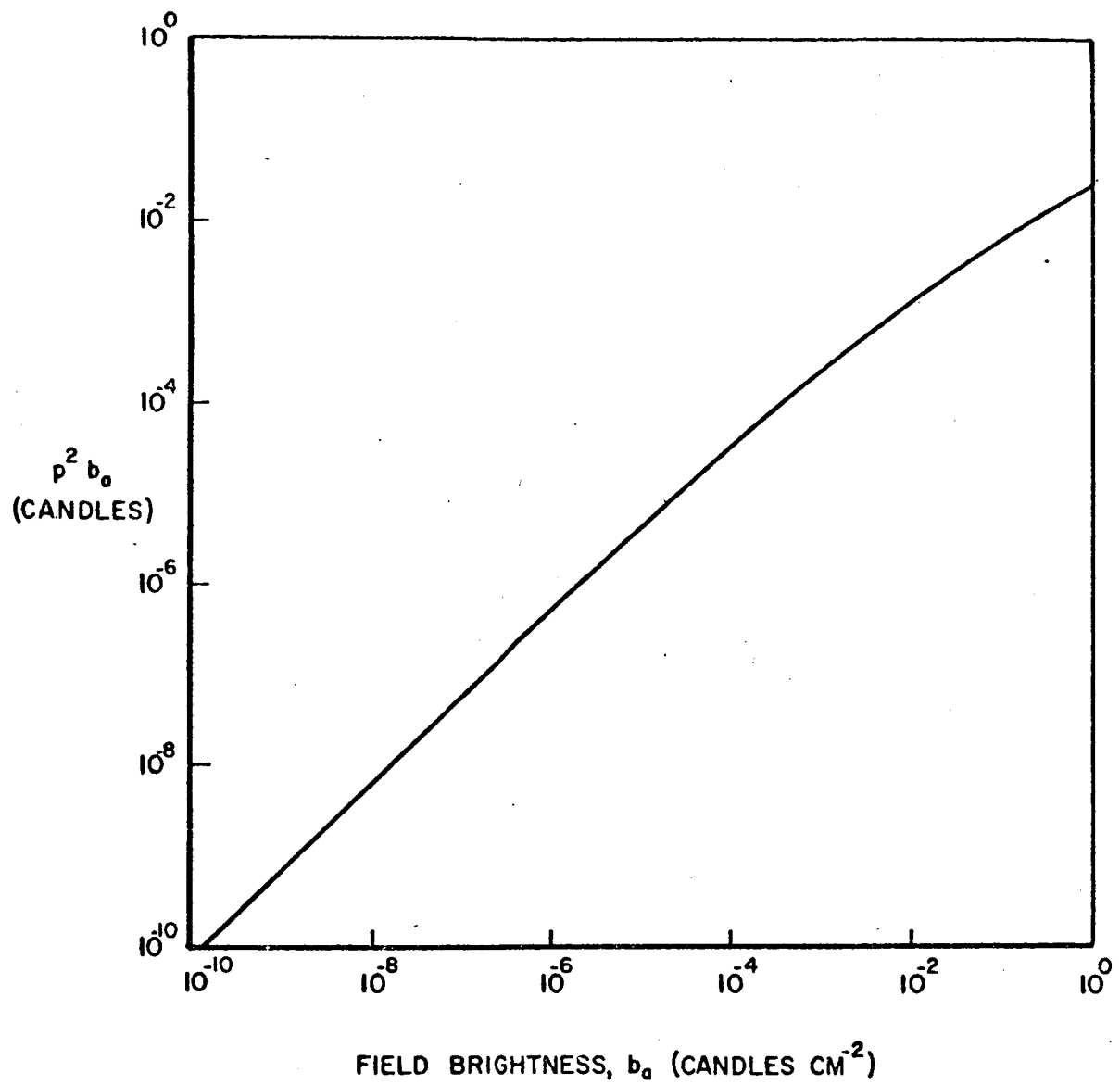
Assuming a perfect optical system, two causes of the enlargement of a point source must be considered. The first is diffraction, which for the case at hand produces an image of diameter δ minutes of arc in accordance with the equation

$$(13) \quad \delta = 0.461 \text{ M/D},$$

where D is expressed in centimeters. An inspection of Figure 11 indicates that as long as the apparent spot diameter is less than about 3 minutes of arc, little degradation of threshold performance is to be expected. This partially accounts for the condition $M = 16 \text{ D}$ (in inches) mentioned by Hastings⁷ and used by Dole. The second effect, which becomes important at moderately high magnifications, is astronomical seeing. Because of atmospheric turbulence, the disk of a star subtends, under average conditions, about 3 seconds of arc. At magnifications on the order of 100 to 200, the detection performance of a telescope begins to be degraded at low light levels by this effect.

The diameter of the pupil of the eye, p , appearing in equations (11) and (12) is a function of the brightness level (Figure 12). Following Dole³,

⁷ C. S. Hastings, "Telescope Oculars," Amateur Telescope Making, Book One, Scientific American, 1955.



A-175

Fig. 12 Response of the Pupil of the Eye to Brightness Level (After Dole³)

we may rewrite equation (12) as

$$(14) \quad b_a p^2 = t d^2 b$$

and equation (11) as

$$(15) \quad i = \frac{1a}{t} \left(\frac{p}{D} \right)^2.$$

Setting $t = 0.8$ and $M = 16 D$ (inches), $d = 1/16$ inch = 0.15875 cm, and

$$(16) \quad b_a p^2 = 0.02015 b.$$

Noting that, according to Tousey and Hulburt⁶, at the threshold a star can only be found with difficulty, while from 2.5 to 5 times the threshold it is only moderately hard to find, we will solve for $3 i_a$,

$$(17) \quad i = 3.75 i_a \left(\frac{p}{D} \right)^2.$$

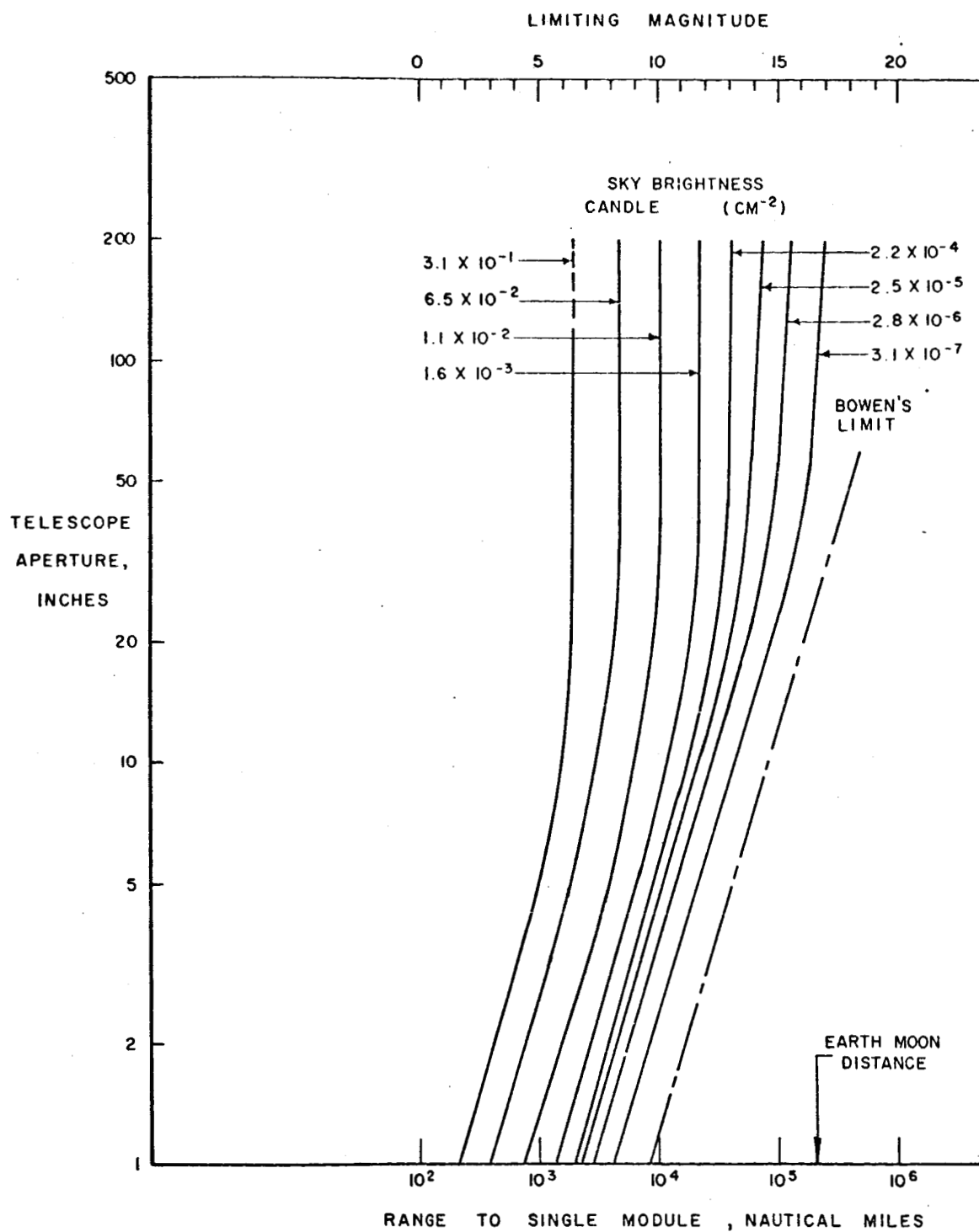
The diameter of the seeing disk is taken as 3 seconds of arc. The apparent diameter δ_a of the disk is thus

$$(18) \quad \begin{aligned} \delta_a &= M \\ &= 0.8 D \end{aligned}$$

where D is measured in inches.

Figure 13 indicates the limiting magnitudes of various visual instruments as a function of background brightness, assuming the above conditions. For purposes of ready reference, the range to a single module, using the 30% reflectivity curve of Figure 7, has also been indicated.* The line labeled "Bowen's Limit" refers to the equation:

* It should be noted that no correction has been assumed for extinction.



A-176

Fig. 13 Limiting Magnitudes of Visual Telescopes with
 $M = 16$ D Inches, Moderate Ease of Certain Detection
 3 Second of Arc Seeing Disk Diameter

$$(19) \quad M = 9.46 + 5 \log D,$$

where D is the aperture in inches. For the conditions of the problem (M = 16 D inches), this satisfies Bowen's equation.

$$(20) \quad M = 6.52 + 2.5 \log D + 2.5 \log M,$$

which has been empirically found to represent the limiting visual magnitude against a dark sky of telescopes less than 60 inches in aperture over a wide range of magnifying powers, provided the magnification is sufficiently small so that the image diameter is not important.⁸

An inspection of Figure 13 reveals the following points of interest:

1. For a background brightness equivalent to the mean brightness of the full moon (2.5×10^{-1} candle cm^{-2}), little or no gain in limiting magnitude is achieved by increasing the aperture above 20 inches diameter. Under these conditions, the limiting magnitude is approximately 6.2, or about 1.3×10^4 brighter than a single 30% reflective module at the distance of the moon.
2. For a background brightness equivalent to the mean brightness of the quarter moon (5.5×10^{-2} candle cm^{-2}), the "optimum" aperture is about 30 inches

⁸

I. S. Bowen, Publications of the Astronomical Society of the Pacific, 59, 253, 1947.

diameter, and the limiting magnitude is about 8.2, some 1.6×10^3 brighter than a single module at the distance of the moon.

3. For a background brightness of 5×10^{-6} candle cm^{-2} , corresponding to the aureole 0.3 degree from the full moon, little gain can be expected beyond a 50 inch aperture and a limiting magnitude of about 14.5, some 6 times brighter than that of a single module at the range of the moon.
4. For a background brightness of 3×10^{-7} candle cm^{-2} , corresponding to the aureole 0.8 degree from the quarter moon, a 60 inch telescope would allow us to detect a single module.

These results are necessarily tentative, and neglect extinction, which for moderate zenith distances would decrease the effective range by a factor of 1/2 and increase the amount of light required for detection by a factor of 1.4

b. Photography

The granular nature of the photographic emulsion places a limit upon the faintest image detectable against a background. In order to insure that the image is distinguishable from the point-to-point fluctuations of the background, the number of grains required in the image due to the source to be detected should exceed the RMS fluctuation of the background within the image area by a coefficient of certainty, that is,

$$(21) \quad S = k(\bar{g})^{\frac{1}{2}}$$

where S is the number of grains in the image due to the source and \bar{g} is the average number of grains per image area. The coefficient of certainty, k , must be equal or greater than 5 if, within an area of the size typically covered by an astronomical photograph, none of the noise peaks is to be confused with faint images.

Proceeding from such a threshold criterion, Baum^{9, 10} has shown that, for an unsaturated exposure, the threshold magnitude is given by

$$(22) \quad m = \text{Constant} + 0.5m_{\text{sky}} - 2.5 \log_{10} \alpha - 2.5 \log_{10} k \\ + 1.25 \log_{10} (D^2 qT) - 1.25 \log_{10} (1 + R),$$

where

α = Angular diameter of the stellar image or of an image element,

q = Average effective quantum efficiency,

T = Effective integration time,

and

R = Ratio of instrument background to sky background.

The constant accounts for the conversion of units (from the average number of eligible photons sec^{-1} received per unit area from a unit solid angle of the sky background to the magnitude of the sky, m_{sky} , per unit solid angle).

⁹ W. A. Baum, "The Detection of Faint Images Against the Sky Background", Transactions of the International Astronomical Union, 9, 681, 1955.

¹⁰ W. A. Baum, "The Detection and Measurement of Faint Astronomical Sources", in Astronomical Techniques (W. A. Hiltner, editor), University of Chicago Press, 1962.

Equation (22) applies to photoelectric, visual, and photographic observations, provided saturation does not occur. Indeed, as Baum has pointed out,¹⁰ equation (20) is but a special case of this expression. If everything else is held constant, equation (22) indicates that the threshold magnitude will be decreased by one magnitude if the sky becomes two magnitudes brighter or if the image diameter increases by a factor of 2.512.

When the detector becomes saturated, as is more often the case photographically, the relevant equation is

$$(23) \quad m_l = m_{sky} - 2.5 \log_{10} \alpha - 2.5 \log_{10} k + 2.5 \log_{10} f \\ + 1.25 \log_{10} E - 2.5 \log_{10} (1 + R),$$

where

f = focal length of the system

and

E = maximum number of statistically effective
photo-events that can populate a unit area
at the focus.

In this event, the limiting magnitude varies directly as the sky background. It is interesting to note that the aperture of the telescope, the integration time, and the quantum efficiency of the detector do not appear in equation (23), provided, of course, that statistical saturation is reached (the required integration time does, of course, depend on the aperture and the quantum efficiency).

The photographic image of a distant point is degraded by a number of effects. Even if the optical system is perfect, the angular diameter of the smallest image is approximately

$$(24) \quad \alpha = S + 1.2\lambda/D + \Delta/f,$$

where S is the angular diameter of the seeing disk, λ is the wavelength of the exposing light, Δ is a characteristic of the emulsion, and f is the focal length of the telescope. Reasonable values of S and λ are three seconds of arc and 5000 Å. Thus, even for a 10 cm objective the diffraction term ($1.2\lambda/D$) is small compared to the seeing. The value of Δ varies from emulsion to emulsion, and is dependent on the wavelength of the exposing light and the density of the image. For fast blue sensitive emulsions, such as would probably be used, and for threshold images, Δ is on the order of 20 to 30 microns. Thus, for telescopes with focal lengths less than one or two meters, Δ dominates, and equation (23) may be written:

$$\Delta/f \geq S$$

$$(25) \quad m_l = m_{\text{sky}} - 2.5 \log_{10} \Delta - 2.5 \log_{10} k \\ + 5 \log_{10} f + 1.25 \log_{10} E - 2.5 \log_{10} (1 + R).$$

For longer focal lengths, S dominates, and may be substituted directly into equation (23). When near the limit photographically, R is small and may be neglected.

Figure 14 displays curves of equations (23) and (25) for $\Delta = 25\mu$, $S = 3$ seconds of arc, $E = 5 \times 10^6$ grains cm^{-2} , and $k = 5$. The magnitudes

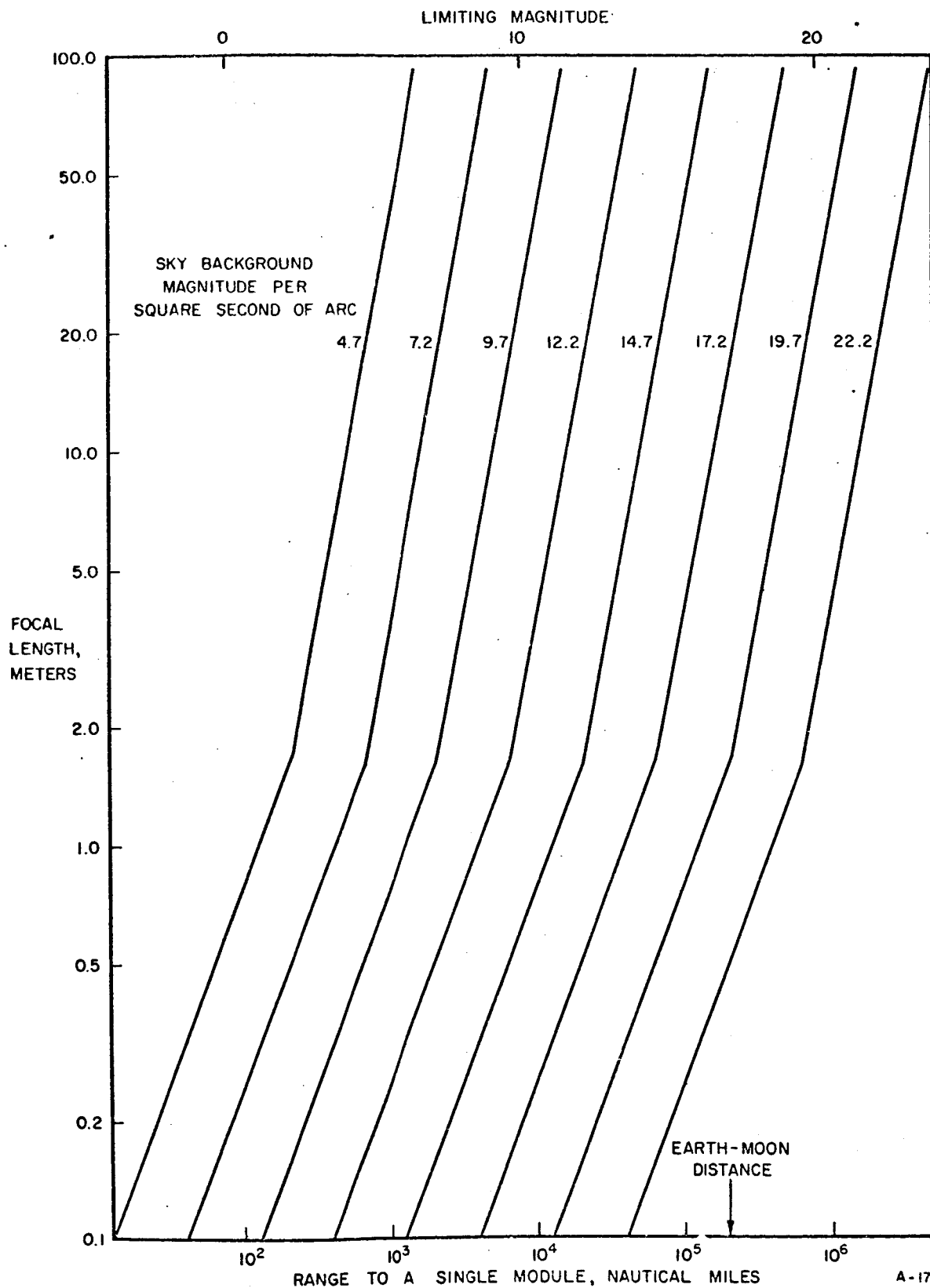


Fig. 14 Limiting Magnitudes of Photographic Telescopes,
 $\Delta = 25$, $\alpha = 3''$, $E = 5 \times 10^6$, $k = 5$

indicated on this figure are photographic, and in interpreting them in terms of Sections 2.1 and 2.2, allowance must be made for the colors of the various sources. The sun, for instance, is about 0.4 magnitude fainter on the photographic scale than it is on the visual. This fact is usually expressed by saying the sun has a color index of +0.4 magnitude. The moon and the night sky have color indices of +0.8 magnitude, as does the moon's aureole at the limb of the moon. At a distance of 15° from the limb of the moon, however, the aureole is bluer, having a color index of perhaps +0.5. A perfectly white target illuminated by the sun would have a color index of +0.4 magnitude. Thus, the photographic magnitude of such a target would be 0.4 magnitude greater than the visual magnitude. A color index of +0.5 has been assumed in the construction of the range to a single module scale of Figure 14, which refers to a 30% reflecting target. Atmospheric absorption has again been neglected. Thus, the ranges may be decreased by a factor of up to $1/4$, and the amount of light required for detection may be increased by a factor of 2 (0.8 magnitude) at a zenith distance of 60° .

An inspection of Figure 14 reveals the following points of interest:

1. For a background brightness equivalent to the mean brightness of the full moon (2.5×10^{-1} candle = $3.7 \text{ m}_v \text{ second}^{-2}$ of arc = $4.5 \text{ m}_{pg} \text{ second}^{-2}$ of arc for a color index of +0.8), the detection of a single module at the distance of the moon would require a fantastic focal length (on the order of 2×10^6 meters).

For a reasonably large focal length, say 15 meters, the limiting magnitude is some 12.8 magnitudes, or a factor of 1.3×10^5 , too bright.

2. For a background brightness equivalent to the mean brightness of the quarter moon (5.5×10^{-2} candle $\text{cm}^{-2} = 5.4 m_v \text{ seconds}^{-2}$ of arc $= 6.2 m_{pg} \text{ second}^{-2}$ of arc for a C.I. of +0.8), the required focal length is on the order of 4×10^6 meters, still much too large for practical consideration, while for a 15-meter focal length, the limiting magnitude is 10.9 magnitudes or 2.2×10^4 times too bright to detect a single module on the moon.
3. For a background brightness of 5×10^{-6} candle cm^{-2} ($16.2 m_{pg} \text{ second}^{-2}$ of arc for a C.I. of +0.8), corresponding to the aureole 0.3 degree from the full moon, a single module, at the distance of the moon can be detected with a telescope of focal length 39 meters. A 15-meter focal length instrument falls 0.9 magnitude short of detecting the target.
4. For a background brightness of 3×10^{-7} candle cm^{-2} ($=19.3 m_{pg} \text{ seconds}^{-2}$ of arc for a C.I. of +0.8), corresponding to the aureole 0.8 degree from the quarter moon, a single module at the distance of

the moon could be detected photographically with
a telescope of about 2.4 meters focal length.

So far we have investigated only the question of whether or not a telescope of a practical focal length could photograph a given target against a given background. It remains to be seen whether or not the limiting magnitudes could be reached in a reasonable time with a reasonable aperture. This involves a consideration of the quantum efficiency of the detector, and it is, therefore, necessary to convert magnitudes into photons per second per unit area of aperture.

Making use of the fact that a star of $m_v = +0.8$ is equivalent to a unit candle power source at 1 km, or that a star of zero visual magnitude is equivalent to a 2.08 candle power source at 1 km, one may readily calculate that a zero magnitude star is equivalent to an illuminance of 2.08×10^{-10} lumen cm^{-2} . At the maximum of the visual luminosity curve ($\lambda = 5550 \text{ \AA}$), the mechanical equivalent of light is 685 lumen/watt, and thus a zero visual magnitude star is equivalent to an illuminance of 3.04×10^{-13} watt cm^{-2} . The equivalent width of the visual luminosity curve is 1070 \AA . Thus, the illumination of the optical system at $\lambda = 5550 \text{ \AA}$ by a star of zero apparent magnitude is approximately 2.84×10^{-16} watt $\text{cm}^{-2} \text{ \AA}^{-1}$. The energy, in joules, of a photon of wavelength λ is given by $E = hv = hc/\lambda$, which at $\lambda = 5550 \text{ \AA}$ is 3.58×10^{-19} joule/photon. Thus, at 5550 \AA , a star of zero magnitude is equivalent to 7.94×10^2 photons $\text{second}^{-1} \text{ cm}^{-2} \text{ \AA}^{-1}$.

Figure 15 indicates the photon flux from a 6000°K zero magnitude black-body, approximating the sun's temperature. The photographic magnitude of

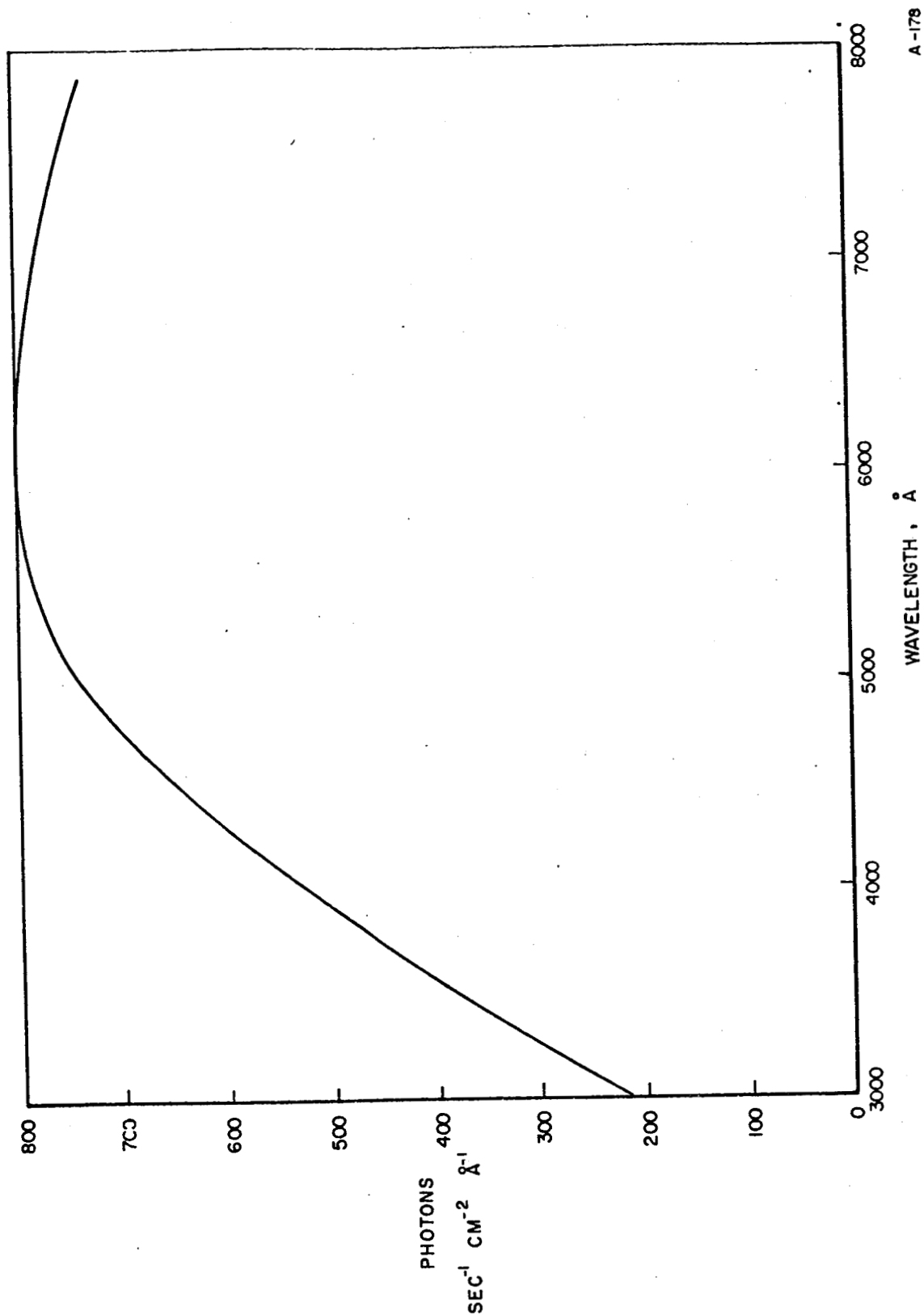


Fig. 15 Photon Flux Through an Aperture
from a 6000°K $m_v = 0.0$ Source

such a body is approximately +0.4. This refers to a telescope-emulsion combination with a maximum sensitivity at about 4600 \AA and an equivalent width of about 1290 \AA . From Figure 15 the photon flux at 4600 \AA received from a $0.4 m_{pg}$ source is about $670 \text{ photons second}^{-1} \text{ cm}^{-2} \text{ \AA}^{-1}$, or about $8.65 \times 10^5 \text{ photons second}^{-1} \text{ cm}^{-2}$ are available for exposing the photographic plate.

A single 30% reflecting module at the distance of the moon is of the 17th photographic magnitude. For the photographic system so far considered, we therefore receive about $2 \times 10^{-1} \text{ photons second}^{-1} \text{ cm}^{-2}$. From the sky considered in example 4 above ($19.3 m_{pg}$ per square second of arc) we receive about $2.4 \times 10^{-2} \text{ photons second}^{-1} \text{ cm}^{-2}$ per square second of arc. For a telescope with a focal length greater than 1.67 meters, the image of the module subtends 3 seconds of arc, or about 7 square seconds of arc. In such a case, the sky background contributes $1.7 \times 10^{-1} \text{ photons second}^{-1} \text{ cm}^{-2}$.

The total number of photoevents due to the star will be

$$(26) \quad S = nAqt$$

where n is the number of available photons, A is the area of the aperture, q is the quantum efficiency, and t is the exposure time. Similarly, the number of grains due to the background is

$$(27) \quad g = NAqt + 3$$

where N is the number of available background photons for the solid angle

subtended by the target and β is the inherent background fog over the same solid angle. Obviously, β depends on the focal length. Equation (21) may then be rewritten

$$(28) \quad nAqt = k (NAqt + \beta)^{\frac{1}{2}}$$

The value of q for a given photographic emulsion varies with the exposed density of the emulsion. Astronomical experience indicates that a value of 0.002 is realistic for full exposures with fast emulsions. Within a 25μ image, such as we would encounter with a matched system of $f = 1.67$ meters, perhaps 25 grains are due to chemical fog. Then detection requires

$$4 \times 10^{-5} At = 5 (3.4 \times 10^{-5} At + 25)^{\frac{1}{2}}$$

where A is in cm^{-2} and t is in seconds. Thus, $At \approx 9.4 \times 10^5 \text{ cm}^2 \text{ seconds}$. For reasonable f /ratios, the aperture of a 1.67 meter $f.l.$ objective would not exceed 1 meter, or $A \leq 7.8 \times 10^3 \text{ cm}^2$. Thus $t \geq 120$ seconds, a not unreasonable exposure time.

It then appears possible to photograph a single module in the vicinity of the moon with a fairly large aperture in a reasonably short time. This of course presupposes that the motion of the module can be compensated for. If the module were sufficiently bright, then photography of the module under more adverse background illumination conditions, as for instance, against the full moon, also becomes reasonable. A more detailed analysis is required to specify exact exposure times required.

c. Television Techniques

The photocathode of an image tube may be thought of as a mosaic of resolution elements in a manner analogous to the procedures used in treating the photographic emulsion. Thus, for the unsaturated case, equation (22) applies, while the saturated case, representing the ultimate threshold of the system, is described by equation (23).

Three basic types of television tubes are available commercially: the C.P.S. Emitron (or Orthicon), the Image Orthicon, and the Vidicon. The modes of operation and differences between these devices are beyond the scope of this report. Results of various investigations^{11, 12} tend to rule out present day Emitrons and Vidicons and favor the newer, improved Image Orthicons for applications of the type being considered.

As has been mentioned previously, the effective quantum efficiency of a photographic emulsion is about 0.2% for background limited exposures. Under similar conditions, the quantum efficiency of a photocathode may be on the order of 10%. Thus, if subsequent degradation of the signal is ignored, the fundamental quantum advantage of a photocathode over photographic emulsion may be as large as a factor of 50. Unfortunately, however, merely increasing the quantum efficiency alone does not gain us anything as far as the limit of detection is concerned, although of course,

¹¹ J. D. McGee, "Image Detection by Television Signal Generation", in Astronomical Techniques, (W. A. Hiltner, editor), University of Chicago Press, 1962

¹² R. K. H. Gebel, Limitations in Detection of Celestial Bodies Employing Electronically Scanned Photo-conductive Image Detectors, ARL 153, Aeronautical Research Laboratory, Office of Aerospace Research, U.S.A.F., Wright-Patterson Air Force Base, Ohio.

it will allow us to reach the limit with a shorter exposure for a given aperture.

Unlike the case of the photographic emulsion, the inherent noise of an image orthicon becomes important. To be primarily considered is the electron noise inherent in the scanning beam. As the output signal of the tube is such that the maximum current refers to the faintest signal, the situation is unfavorable from the standpoint of quantum statistics. As late as 1955, it was estimated¹³ that the initial photoelectron flux of an orthicon needs to be multiplied by a factor of 200 to 300 in a relatively noise-free way before it is read by the electron beam, if the fundamental threshold set by photoelectron statistics is to be met. Later tubes, and particularly the intensifier orthicon, have improved this situation.

Gebel¹⁴ has employed a two-stage intensifier having a primary amplification of 100, which in a diffraction limited matched system (i.e., $\Delta \approx 1.2 \lambda f/D$) is day sky background limited, the ratio of scanning noise to background noise being about 1/4. The performance of this system using a 10-inch telescope and a 1 second integration time, as predicted by Gebel, for $k = 1$ is such that an 11.6th magnitude object should be detectable against a daylight sky. For $k = 5$ and for a 3 second of arc seeing disk,

¹³ G. A. Morton, "Information Storage and Integration Applied to Low-Contrast Astronomical Images", Transactions of the International Astronomical Union, 9, 676, 1955.

¹⁴ R. K. H. Gebel, Daytime Detection of Celestial Bodies Using the Intensifier Image Orthicon, WADC TN 58-324, Wright Air Development Center, 1958.

as we have been assuming in the previous examples, this limiting magnitude is reduced to about magnitude 8. One might then naively suppose that by increasing the magnitude of the background by ΔM , one increases the limiting magnitude by either $0.5 \Delta M$ or ΔM , depending on whether saturation is reached or not. However, one must note that as the background is decreased, the ratio of noise due to the scanning beam increases and the latter eventually becomes the limiting noise. As the ratio of background noise to scanning noise is, according to Gebel, but 4 for daytime operation, this particular system should become scanning noise limited when the background has decreased to about $1/16$ its daytime value, or by 3 magnitudes. For a non-saturated system, this corresponds to a limiting magnitude of 9.5, for a 1-second exposure with a 10-inch telescope under the above conditions, no matter how faint the sky becomes. This limit may, of course, be altered by changing the system parameters D , f , and/or t .

Aside from the limitation produced by the noise due to the mechanism of an orthicon, attention must also be paid to the resolution of these devices, which is considerably poorer than that found in photographic emulsions. Manufacturer's data indicate resolutions on the order of 5 to 10 line pairs per mm (10 to 20 TV lines per mm) for low light levels and long integration times, an order of magnitude poorer than that of photographic emulsions. As the integration time is increased, or as the background light level is decreased, the resolution becomes poorer. This also complicates the application of equations (22) and (23). It may be remarked at this time that, for the recognition of parallel line test targets of 100% contrast, manufacturers find an improvement in resolution with longer integration times,

although astronomical tests indicate the opposite. In connection with another project, W. A. Baum has supplied the data in Table II, based on tests conducted by the Mount Wilson and Palomar Observatories, in 1959 and 1960, in cooperation with the Smithsonian Astrophysical Observatory, E. R. D. L. (U.S. Army), and the Princeton R.C.A. Laboratory.

Summaries of other astronomical tests of image orthicons and other image tubes may be found in the reports of Subcommittee 9a of the International Astronomical Union.¹⁵

TABLE II

Values of the Resolution of Image Converters as a Function of Integration Time When Exposed to a Moonless Night Sky.*

Integration Time	Mfr. Data Z-5294 at F/1.5	Palomar Z-5294 at F/12	Mfr. Data C-74034 at F/1.5	Palomar Intens. 0 at F/12
0.033 Sec.	4.4 p/mm	--- p/mm	9.0 p/mm	5.0 p/mm
0.02	5.6	---	---	---
1.0	6.6	4.0	---	4.2
4.0	---	3.6	---	3.7
16.0	---	2.7	---	---

* Assuming optical transmission of 60% and maximum raster width (36 mm). Scanning (reading) rates standard (1/30 sec.).

Returning for a moment to the 10-inch diffraction limited matched system discussed above, it is interesting to note that a resolution of even 10 line pairs mm^{-1} would dictate a focal length of 40 meters, and that at this focal length, the field of view corresponding to a 45 mm diameter

¹⁵ Report of Sub-commission 9a (Image Converters) of the International Astronomical Union, Transactions of the International Astronomical Union, 10, 143, 1958 and 11, 1962.

photocathode would be only 4 minutes of arc in diameter.

Table III lists values of the limiting visual magnitude as a function of integration time, as achieved in the Palomar tests, using the Cassegrainian focus of an F/12, 20-inch aperture reflector against a moonless dark sky. These values are plotted in Figure 16.

TABLE III

Threshold Magnitudes of Image Tubes,
20-inch f/12 Telescope.*

Integration Time	Threshold m_v , Z-5294 (MgO ₂ Target Image Orthicon)	Threshold m_v , Glass Target Intensifier Orthicon	Threshold m_v , MgO ₂ Target Intensifier Orthicon
0.033 Sec.	----	11.9	12.5
0.067	----	----	13.0
0.125	----	12.7	----
0.50	----	13.5	14.0
1.0	13.5	13.9	14.3
4.0	14.9	14.3	14.3
16.0	16.2	14.5	----

* Cooled tubes read at normal rate (1/30 sec.) at end of integration time.

A number of interesting points may be inferred from Figure 16. First, the f/ ratio of the telescope used (f/12) was sufficient for the intensifier orthicons to become sky noise limited, as in the case of the daylight-sky instrument previously discussed, while the image orthicon is being intrinsically limited. This may be deduced from equation (28), by noting that for the intensifiers, a 6-fold increase in exposure time is required to gain one magnitude, while for the image orthicon, only a 2.5-fold

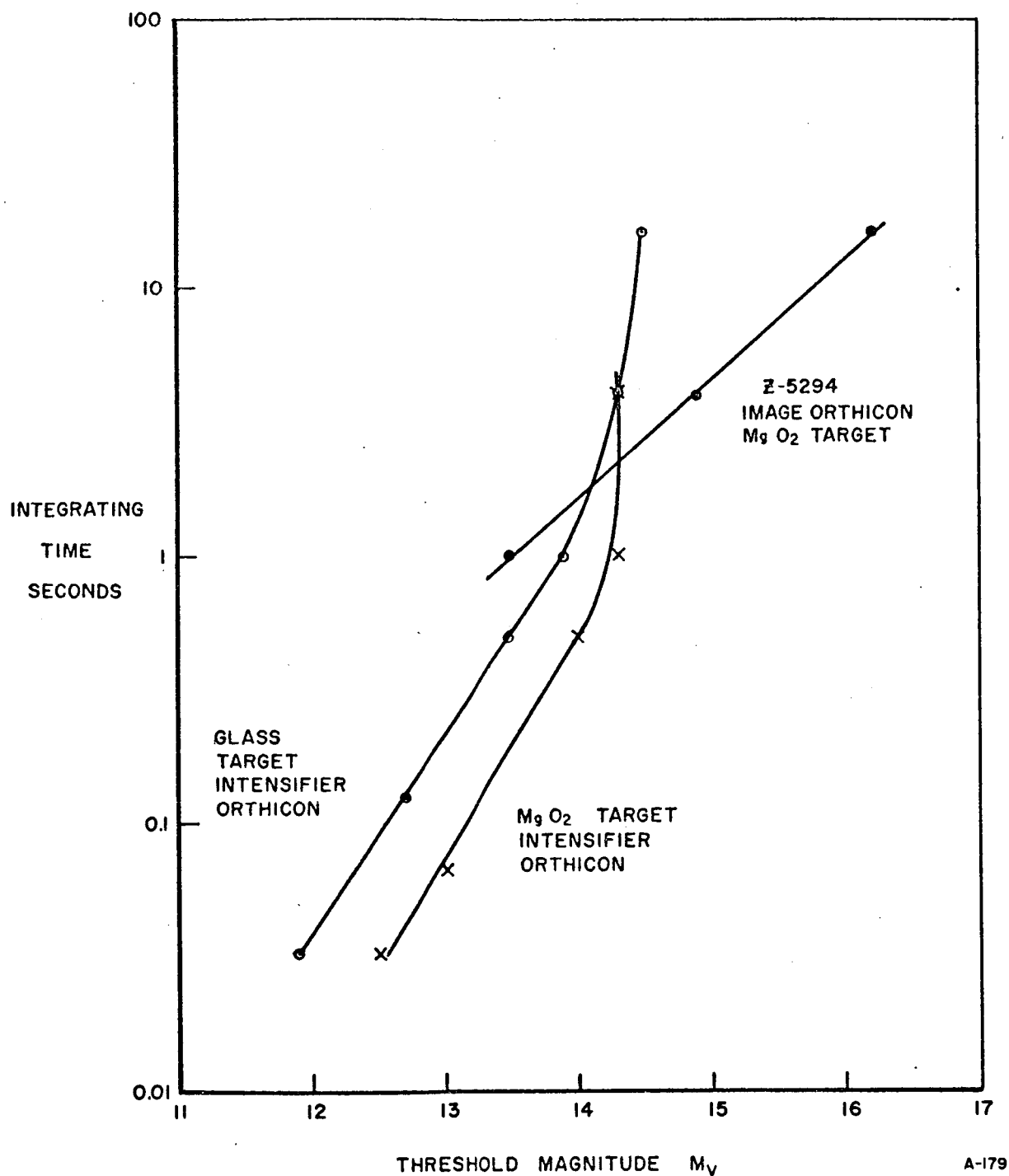


Fig. 16 Performance of Image Tubes Against a Dark Sky with 20-inch Aperture, $f/12$. (Data from Table II)

increase is required. This is because, in the intensifier orthicon, a very small number of primary photoelectrons can change the orthicon storage target to the "knee" of the characteristic curve, where the signal ceases to be proportional to the incident illumination.* The signal-to-noise ratio may therefore be determined mainly by this small number of primary photoelectrons, which for moderate resolution work would be very small even at saturation.¹¹ The answer is, of course, to use such devices at even poorer resolutions than image orthicons. This allows a larger primary signal per picture element increase in signal-to-noise ratio.

Secondly, saturation is reached in the case of the intensifier orthicons at about magnitude 14.5. This seems reasonable in view of the fact that an intensifier orthicon at maximum resolution may have a dynamic range of the order of a factor of 10 in brightness (2.5 magnitudes). Image orthicons, on the otherhand, may cover a range several times this.

It may be noted that, for some tubes, the integration time is limited by the leakage of the charge from the target. This may be thought of as somewhat akin to photographic reciprocity failure, although the mechanism is different. For some storage target materials, pronounced image deterioration occurs in extremely short times. MgO_2 is a pronounced exception. DeWitt¹⁶ has reported that with a cooled image orthicon of this type,

¹⁶ J. H. DeWitt, Loc cit reference 15, Volume 11.

* This illustrates perhaps another fundamental difference between the photographic process and photoelectric techniques. That which photographers refer to as the "shoulder" of the characteristic curve, electronics engineers designate the "knee". Casual research through a large body of texts (numbering several digits) has not uncovered a similar electronic synonym for photography's "toe". On this portion of the anatomy, both technologies appear in agreement.

integration times amounting to tens of minutes (rather than seconds or less) may be achieved without image deterioration. For standard glass-target orthicons, operation at low temperature is required. At -75°C , integration times of a few hundred seconds are possible.¹⁷

Referring again to Figure 16, let us consider the behavior of the image orthicon. As has been stated, we may infer from the figure that the orthicon is limited intrinsically. This limitation is imposed by the shot noise of the scanning beam. Since the modulation of this beam is inefficient, being 20% at most, it is necessary to provide a scanning beam some 2 to 10 times more intense than the signal current which has charged the storage target. As a result, the beam noise, which is a maximum in the dark areas of the picture, decreases by only about 5 to 10% in the white areas, and acts as a source of noise which is relatively dependent of the background signal. Thus, if i is the signal current, the beam current is

$$(29) \quad i_b = \frac{i_{\max}}{\eta},$$

where η is the modulation factor.

The return current in the beam is

$$(30) \quad i_{\text{ret}} = i_b - i,$$

and the associated shot noise is

$$(31) \quad \bar{i}_{\text{ret}} = (2ei_{\text{ret}} \Delta f)^{\frac{1}{2}}$$

where e is the electronic charge and Δf is the bandwidth of the measuring circuit.

¹⁷ W. Livingston, Publications of the Astronomical Society of the Pacific, 69, 390, 1957.

The noise in the current charging the target depends upon the number of photoelectrons involved, and is at a maximum when the tube is saturated. The technique of charge storage is a charge integration method, rather than a current measuring method. If the primary photocurrent is i_p the statistical noise inherent in the charge is

$$(32) \quad \overline{i_p t} = (e^{-1} i_p t)^{\frac{1}{2}}$$

where t is the integration time involved in building up the charge. The primary photocurrent may be amplified by one or more stages of multiplication, as in the intensifier orthicon, and additionally the secondary yield of the target plate must be considered. Assuming that these effects do not degrade the signal-to-noise performance of the system, the noise associated with the charge at the target is

$$(33) \quad \overline{it} = (e^{-1} i_p t)^{\frac{1}{2}} V (S-1) ,$$

where V is the multiplication of the intensifier and S is the secondary yield of the target plate. We note that the charging current i is

$$(34) \quad i = V (S-1) i_p .$$

The ratio of the two noise sources is, from equations (31) and (33)

$$(35) \quad \frac{\overline{i_{ret}}}{\overline{it}} = \frac{(2e i_{ret} \Delta f)^{\frac{1}{2}}}{(e^{-1} i_p t)^{\frac{1}{2}} V (S-1)} ,$$

which may be rewritten in accordance with equations (29), (30) and (34) as

$$(36) \quad \frac{\overline{i_{ret}}}{\overline{it}} = \frac{(2e^2 [i_p \max - i_p] \Delta f)^{\frac{1}{2}}}{(i_p \eta V [S-1] t)^{\frac{1}{2}}}$$

For a tube requiring exposure to a relatively large light level to reach saturation, far from saturation, and with a large bandpass, scanning noise dominates. On the other hand, background noise dominates near saturation in a tube with a large modulation factor, high intensification gain, and long integration time. McGee¹¹ estimates that $\overline{i_{ret}} / \overline{it} \approx 1.5$ for normal operation of a typical image orthicon, near saturation. As pointed out above, for an intensifier orthicon, this ratio is near 1/4.

Because of the large number of complications involved in accurately predicting the threshold of television systems, we shall for the present not attempt such an analysis. Ignoring for the moment the effects of integration time and bandwidth, and accepting a figure of 0.2 mm as the size of the smallest resolvable element on the photocathode, we shall solve equations (23) and (25) for a statistically saturated case. For telescopes with focal lengths less than 12.4 meters, the resolution of the tube dominates, while for longer focal lengths, the 3 second-of-arc seeing disk becomes important. In the case of an image orthicon, about 600 primary photoelectrons are required for saturation, while for the intensifier orthicon, perhaps 10 to 20 are necessary. Thus, E may be taken as between 1.5×10^6 and 2.5×10^4 photoelectrons per square centimeter. Figure 17 indicates the performance of a number of saturated image tubes based on such a simplified model. It may be noted that the limiting magnitudes achieved by TV systems is at best only slightly fainter than that found photographically, and it may even be a few magnitudes poorer. The integration times necessary to reach the limit are, of course, much shorter with photoelectric devices.

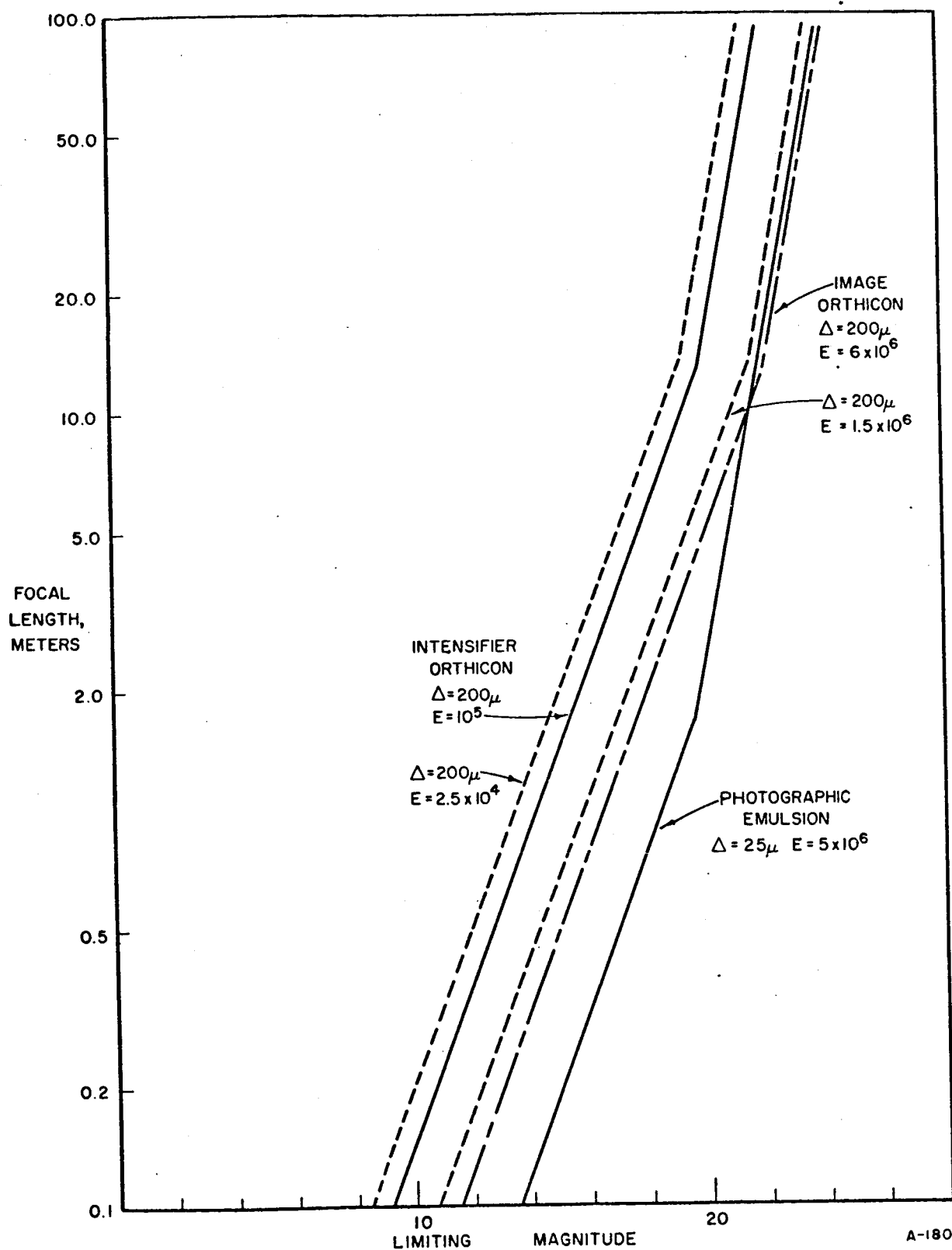


Fig. 17 Limiting Magnitudes of Various Saturated Detectors,
 $M_{\text{sky}} = 22.2 \text{ mag}/\square''$, $S = 3''$, $K = 5$, $R = 0$.

d. Other Detectors

Equations (22) and (23) may be used to describe the performance of other detectors. The most important of these from the standpoint of the Apollo GOSS are infrared detectors. As pointed out in the introduction, a serious problem in passive optical tracking of the Apollo spacecraft during the near earth orbiting phase is introduced by eclipses of the spacecraft.

If a temperature of 350° K is assumed for the vehicle, it would radiate 0.085 watt per cm^2 of surface area. The total energy radiated by the spacecraft (booster and command module) would be in excess of 10^5 watts. For a vehicle at a range of 1000 kilometers, the energy received at a sensor is thus on the order of 8×10^{-11} watt per square centimeter of aperture. Some 50% of this, or 4×10^{-11} watt cm^{-2} , is available in the 8 to 16 micron region. This figure is on the order of the noise equivalent power of typical infrared detectors. It is therefore apparent that infrared techniques could be profitably employed for tracking the vehicle in its near-earth orbit.

2.4 BRIGHTNESS OF OTHER SOURCES.

The faintness of the vehicles in the vicinity of the moon makes it desirable to investigate other sources of illumination. This is done briefly in the following paragraphs.

a. Inflatable Sphere

A possibility is the use of an inflatable sphere, such as the Echo Satellite. Figure 18 indicates the apparent magnitudes of 100% reflecting specular

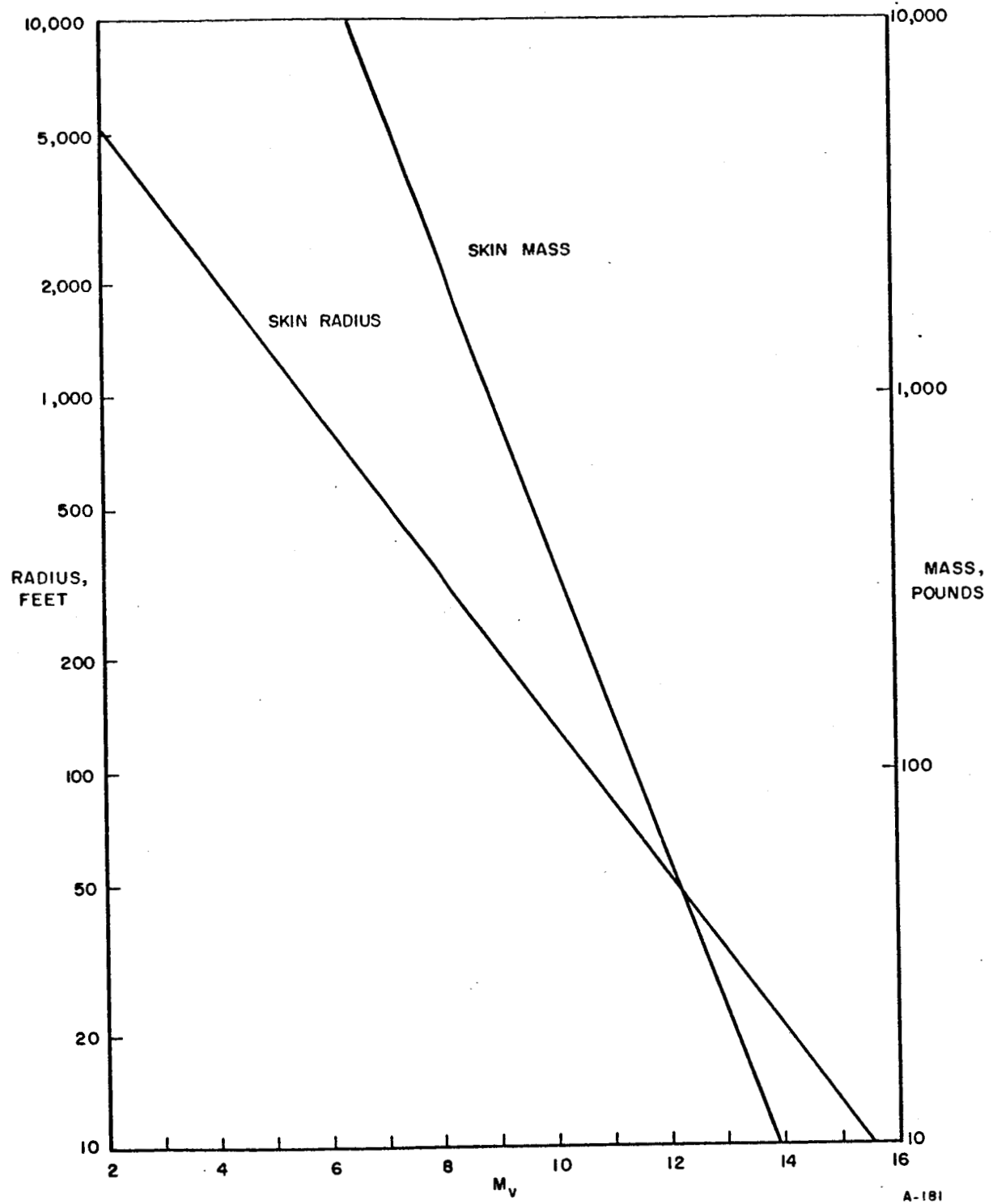


Fig. 18 Radius and Mass of a Thin Film Inflatable Sphere as a Function of Brightness

spheres at the distance of the moon, as calculated from equation (8). The figure also indicates the mass of the skin of such an inflatable, calculated on the assumption that the skin is made up of aluminum foil 1/10,000 inch thick. Buchheim¹⁸ has computed the diameter and mass of a diffuse sphere at full phase, using the same assumptions. Because of the greater brightness of such a target, the required radii and masses are respectively about 1/2 and 1/4 those shown in the figure.

To visually detect such a target against the full moon requires a prohibitively large inflatable (350-750 foot radius and 2,500-10,000 pound mass). Such a device would only prove of value for observations near the full moon, where reasonably small inflatables could materially aid in the detectability of the target.

b. Diffusely Reflecting Plane

Dole³ has investigated the minimum size required of a circular diffusely reflecting plane located on the moon for visual detection from the earth. Unfortunately, as pointed out above, his neglect of the apparent subtense of a "point" image places his results in error. The diameter, D, of a circular diffusely reflecting plane is related to its illuminance, E, by the equation

$$(37) \quad D = 2\rho \left(\frac{E}{E_{\odot} AT \cos \psi} \right)^{\frac{1}{2}},$$

¹⁸

R. W. Buchheim, Artificial Satellites of the Moon, ASTIA Document AD 133021, 14 June 1956. (Rand Corporation Research Memorandum RM-1941).

where ρ is the range to the object
 E_{\odot} is the illumination of the object by the sun
 A is the albedo of the object
 T is the transmission of the earth's atmosphere
 and ψ is the angle between the normal to the surface of the object and the incident radiation vector.

The value of E may be found by reference to Section 2.3.

For the case of specific interest, $\rho = 1.26 \times 10^9$ ft, $E_{\odot} = 1.41 \times 10^4$ lumen ft⁻², $A = 1$, $T = 0.7$ and $\psi = 0^\circ$. For visual detection against a full moon, $E \approx 10^{-9}$ lumen ft⁻². Thus, $D = 800$ ft. Even if a very light material, such as urea-formaldehyde foamed plastic (density 0.1 lb ft⁻³) as suggested by Dole³ were used, the mass of material necessary would prove prohibitive. Spread over an area 800 ft in diameter to a depth of one inch, some 4,200 pounds of material would be required.

c. Specularly Reflecting Plane Mirror

In the case of flat specular reflectors, light is reflected in accordance with the normal law of reflection, and such a surface will be visible by light reflected from a source when it is oriented in such a way that the normal to the surface bisects the vectors defining the directions from the surface to the source and the observer. This angular relationship is extremely critical, and it has even been suggested that use may be made of such a relationship for the accurate determination of the orientation of spacecraft.¹⁹

¹⁹ R. J. Davis, R. C. Wells, and F. L. Whipple, Astronautica Aeta, 3, 231, 1957.

The only source of interest (the sun) is a surface source. The amount of energy reflected to an observer therefore depends on the solid angle subtended at the observer by the reflector (provided it is smaller than the solid angle subtended by the source) and the reflectance of the reflector. At its minimum light, such a surface will appear darker than the interplanetary "sky" it obscures by, say, 5 or 10%, because of reflection losses. The interplanetary "sky" has a brightness of about +23.5 magnitudes per square second of arc, and the specular reflecting plane can be expected to be perhaps 0.1 magnitude per square second of arc fainter at its minimum. The sun has an apparent surface brightness of about -10.5 magnitudes per square second of arc. Provided that the reflecting surface subtends a smaller area than the sun (2.89×10^6 square seconds of arc), the maximum brightness of the surface will be given by

$$(38) \quad m = -12.8 - 2.5 \log_{10} \gamma a + 5 \log_{10} \rho; m \geq -26.8,$$

where γ is the reflectivity of the surface,
 a is the area of the surface in square inches,
 and ρ is the range to the target in nautical miles.

For the most difficult detection problem (a target at the distance of the moon detected visually against the full moon), $m \leq 6.2$. Atmospheric extinction might account for a loss of 0.4 magnitude, and so it is desirable that $m \leq 5.8$. For $\gamma = 0.9$ and $\rho = 210,000$ nautical miles, equation (38) indicates a value of a of 1,600 square inches. A mirror about 45 inches in diameter is thus all that is required. Figure 19 indicates the apparent brightness of such a mirror as a function of its range. Such a

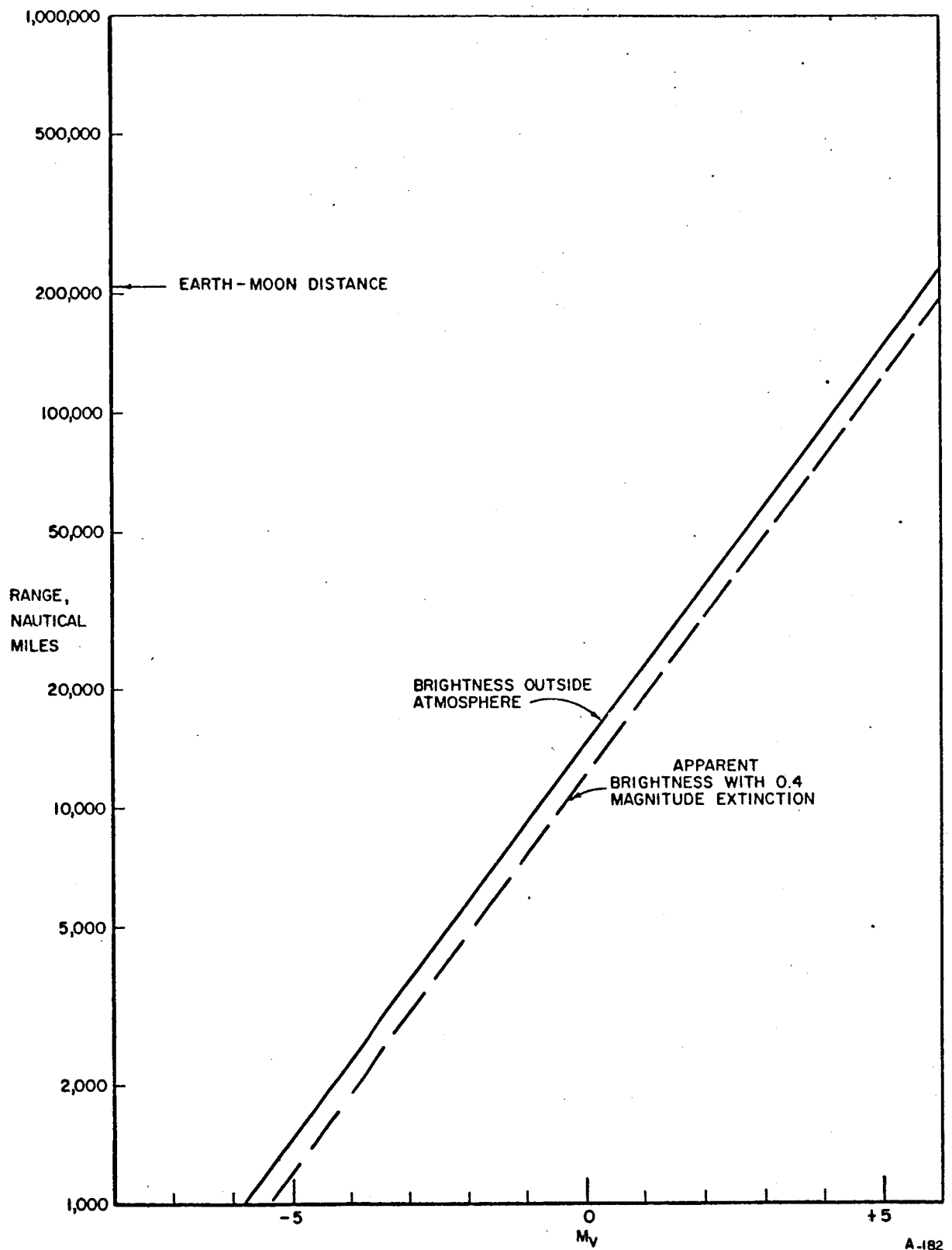


Fig. 19 Brightness of a 45-inch Diameter Flat Mirror as a Function of Distance

target could be detected visually and photographically on or near the full moon. At closer ranges, it would be a spectacular object, visible to the naked eye in broad daylight at ranges less than about 2,800 nautical miles. It would be necessary, however, to provide optical means for the proper alignment of such a target. Perhaps this might be done by some sort of retroreflector sight, as was done with a number of emergency signal mirrors during World War II. If constructed of thin aluminum sheeting, the weight of the mirror would be less than 20 pounds.

d. Fixed Light Emitters

The minimum flux required of, for instance, a searchlight, is simply

$$(39) \quad \phi = \frac{E \rho^2}{T} .$$

The maximum intensity required occurs when $E \approx 10^{-9}$ lumen ft⁻², $\rho = 1.26 \times 10^9$ ft, and $T \approx 0.7$. Then $\phi = 2.3 \times 10^9$ lumen, requiring a lamp of 1.8×10^8 spherical candlepower.

This value assumes that the emitter radiates uniformly in all directions. If a collector, such as a searchlight reflector is employed, the required candlepower becomes much less. If something on the order of 1/3 of the total flux is collected and redirected into a beam with, say, a 5° beam spread, a source of about 10^6 candlepower is required.

GLOSSARY OF SPECIAL SYMBOLS

ϵ	:	projection of β on plane normal to longitudinal axis
β	:	angle between sun direction and observer direction with center of vehicle as apex. This is also called phase angle.
$0^m.0$:	0.0 minutes of arc
z	:	angle from zenith to target
m_v	:	stellar magnitude of vehicle
m	:	threshold magnitude of stellar image
m_l	:	limiting threshold magnitude
C.I.	:	color index
m_{pg}	:	photographic magnitude
h	:	Planck's constant
ν	:	frequency
c	:	velocity of light
p/mm	:	line pairs per millimeter